# ESTIMATION OF SEISMIC RISKS USING STRUCTURAL FRAGILITY FUNCTIONS AND MACROSEISMIC INTENSITY DATA

| AUTHORS | | | REVIEW | | | APPROVAL | | |
|---|---|---|---|---|---|---|---|---|
| NOM | DATE | VISA | NOM | DATE | VISA | NOM | DATE | VISA |
| A. Rosti, M. Rota, E. Fiorini, A. Penna, P. Bazzurro, G. Magenes | | | G. Woo | | | JM. Thiry | | |
| | | | J. Savy | | | G. Senfaute | | |

EUCENTRE®

European Centre for Training and Research in Earthquake Engineering

# RESEARCH ACTIVITY BETWEEN EUCENTRE AND AREVA FOR THE SIGMA PROJECT WP4 TASK 3: DEVELOPMENT AND IMPLEMENTATION OF A METHOD TO COMPARE PSHA RESULTS TO HISTORICAL OBSERVATIONS USING FRAGILITY CURVES



## FINAL REPORT

Prot. No. EUC160/2015U

By

Annalisa Rosti, Maria Rota, Emilia Fiorini,
Andrea Penna, Paolo Bazzurro, Guido Magenes

May, 2015

# TABLE OF CONTENTS

# 1 INTRODUCTION

## 1.1 Foreword

The number of probabilistic seismic hazard analysis (PSHA) studies has been recently increasing, with significant research effort towards the definition of more precise methodologies for the quantification of seismic hazard and the quantification of the related uncertainties. However, there is no consensus yet on these methodologies and on the instruments to be used, whereas there are still very significant uncertainties related in particular to the insufficiency and the inhomogeneous quality of the data, especially in the low to moderate seismicity regions. This results in cases, such as France, for which three different maps were recently established, leading to significant variations in the hazard assessment of the metropolitan territory [e.g. Labbé, 2010].

These are some of the reasons why the scientific and industrial community in France recently agreed on the need for an improvement of the knowledge on PSHA methodologies and of the reliability of PSHA results. This gave birth to the Project SIGMA, which aims at obtaining robust and stable estimates of the seismic hazard in France, by means of a better characterization of the uncertainties involved. As reported by Labbé [2010], in November 2006, the OECD-NEA (Nuclear Energy Agency) convened an expert meeting on Seismic Probabilistic Safety Assessment and issued some recommendations about PSHA implementation, including the fact that "PSHA results should be compared to all available observations, especially for return periods where records are available, in order to get an objective comparison and to improve the confidence in the results, at least in that range of return periods" [OECD, 2007].

Attention was also drawn to the need of verifying and/or validating the ground motion intensity estimates provided by PSHA studies, although there are currently no generally agreed upon criteria for judging the performance of a PSH map [e.g. Stein *et al.*, 2011; Stirling, 2012; Iervolino, 2013]. Several different approaches can be found in the literature for testing PSHA models, often subdivided into the so-called "counting methods" [e.g. Stirling and Petersen, 2006; Albarello and D'Amico, 2008] and the likelihood approaches [e.g. Albarello and D'Amico, 2008]. The different methodologies are briefly presented in Rosti *et al.* [2014] and will not be discussed further here.

Moreover, the comparison of the results of PSHA with observations can be carried out by using observations of very different nature and type, ranging from accelerometric natural or synthetic data, to historical macroseismic observations or evidences related to fragile geological

structures. The main advantages and drawbacks of each of these types of observations will be summarised in the following section. The work described in this report will then concentrate on the use of macroseismic intensity observations, starting from the consideration that in France, as well as in many other countries, more or less reliable historical records, in terms of values of macroseismic intensity, are available on a rather long period of time and these could be used to verify the results of PSHA.

## 1.2 Advantages and drawbacks of the different types of data used for the comparison

According to Beauval [2011], the comparison between PSH hazard curves and observations is meaningful if observations are derived from independent data, i.e. data not directly included in the PSHA. These observations can be of different types, including accelerations recorded by accelerometric stations, "synthetic" accelerations, macroseismic intensities and fragile geological structures. As discussed in some detail in Rosti *et al.* [2014], which includes a quite detailed state-of-the-art of the different approaches used for comparing PSHA results and observation, the use of each type of observation presents advantages and drawbacks.

The use of recorded accelerations could be a natural choice. They are typically affected by a small uncertainty, but the limited lifetime of accelerometric stations, if compared to the long return periods of the major seismic events which may affect the area of interest, makes this option of scarce usefulness. In the case of the South-East quarter of France, indeed, comparisons between observed and predicted occurrence rates at a site are possible only for ground motions with very short return periods and thus they can provide only limited constraints on PSH estimates. Several studies compensated the problem of having too short observation time windows by considering different sites and sampling in space [e.g. Ward, 1995; Albarello and D'Amico, 2008]. However, as discussed in a later section of this report, a limitation of sampling in space can be the non-independence of ground motions at sites affected by the same earthquake. Also, an additional drawback of the use of strong motion data is that these data are not independent from the PSH outputs, since some of them may have been used in the derivation of the adopted ground motion prediction equations (GMPEs) [e.g. Stirling and Gerstenberger, 2010].

An alternative could be the use of synthetic accelerometric data, derived by coupling earthquake catalogues and GMPEs, with the main advantage of enlarging the observation time windows. However, in this case, the results of the comparison are strongly dependent on the reliability of the data from which the synthetic observations are generated and, in particular, a strong assumption has to be made on the choice of the ground motion prediction equation.

Macroseismic intensities, derived from the observation of the effects of an earthquake on the environment, are very approximated measures of the seismic action and unavoidably bear uncertainties and significant subjectivity. Their use also requires a proper characterisation of the seismic vulnerability of structures, in order to establish a link between ground motion intensity measures and corresponding degrees of macroseismic intensity. Despite these limitations, in countries like France, with a long history of civilization, they are available for a long time span and hence allow to enlarge the observation time window and to establish a

comparison between predictions and observations over a longer time period than the accelerometric data.

Finally, fragile geological structures, such as for example precarious rocks, could be used as indicators of unexceeded ground motions, providing direct constraints on the magnitude of ground shaking that has occurred in the area in the past [e.g. Brune, 1996; Purvance *et al.*, 2008]. A combination of the toppling acceleration of these rock structures, which can be derived from field measurements, dynamic tests and modelling, and their age, estimated by means of cosmogenic dating and other methods, allows to constraint the maximum acceleration occurred at the site during the time life of such precarious rocks [e.g. Baker *et al.*, 2013].

## 1.3 Considerations on the SisFrance database of historical seismicity and statistics on the available historical information

As already mentioned, this works concentrates on macroseismic intensity observations, that will be used to carry out comparisons with the results of PSHA.

In particular, the observations reported in the online SisFrance database were used to reconstruct the seismic history of the sites of interest. SisFrance is a database, gathering parametric information on French historical seismicity over about a thousand years, although the time span for the catalogue completeness is significantly shorter. The online database contains information on approximately 6,000 earthquakes felt on the French metropolitan territory or on its near frontiers and reports 1,800 epicentres and approximately 100,000 observations or locations which have suffered earthquakes of varying strengths, with corresponding values of intensity. For each event, Sisfrance provides the date and time in which the earthquake occurred, the nature of the shock (either mainshock, foreshock, aftershock, individual tremor in a swarm or group of tremors in a swarm), the epicentral location (with an associated reliability index) and epicentral intensity. In addition, for each event, a macroseismic data table is available, listing all the sites where that specific earthquake has been felt, with macroseismic observations expressed according to the MSK-64 intensity scale [Medvedev *et al.*, 1964].

A different code is attributed to each macroseismic intensity according to the reliability of the information linked to the observation. Code A means that the reported macroseismic intensity is certain, code B corresponds to a fairly certain intensity, whereas code C means that the reported local intensity is uncertain. In the macroseismic data table, there are also codes qualifying natural phenomena associated with the tremor and observed in the location, including landslides (MT), tsunami (RZ), hydrological effects (EE), "light effects" (PL) and site effects (ES). The presence of such "secondary" effects due to the earthquake may clearly affect the intensity of damage and, hence, the values of macroseismic intensity reported in the catalogue. This issue was taken into account, as will be discussed in a following section of this report.

With specific reference to the area of interest for this study, consisting in the South-East quarter of France and including eleven departments (Alpes Maritimes, Hautes-Alpes, Haute-Savoie, Vaucluse, Savoie, Isère, Rhône, Drôme, Alpes de Haute-Provence, Bouches du Rhône and

Var), the database includes 753 events causing observations in the area of interest. However, the majority of these events has epicentral intensity smaller than or equal to 5, corresponding to cases of no damage. Considering only the events with reported epicentral intensity value, the number of events with epicentre located in France is 603, whereas the number of events with epicentre located outside France is 108. French events are also classified on the basis of the nature of the shock. French mainshocks, with epicentral intensity at least equal to 6 and causing macroseismic observations in the study area, turned out to be 89.

Statistics were also carried out on the number of macroseismic intensities observed in the area of interest, with particular reference to those of engineering interest, i.e. intensities at least equal to 6, which corresponds to slight damage according to the MSK scale. The number of macroseismic observations with intensity at least equal to 6 is about 6.9% (694 observations) of the total number (i.e. 10128 observations). They were produced by 134 independent events.

The number of macroseismic observations with intensity at least equal to 6 due to French events is 521, corresponding to 6.5% of all the macroseismic intensities caused by French events (i.e. 8003 observations). Considering foreign events, the percentage of observations with intensity of at least 6 (173 observations) is about 8.1% of all the observations caused by foreign earthquakes (2125 observations). These figures confirm once more that the large majority of the reported macroseismic observations corresponds to intensity values too low to be of any engineering interest. For higher intensity levels, the majority of the macroseismic observations in the selected area were caused by foreign events.

Table 1.1 summarises the subdivision of the events causing macroseismic observations of intensity at least equal to 6, according to the epicentre location (French and Foreign) and, in case of French events, also based on the nature of the shock (i.e. mainshock, foreshock, aftershock, individual tremor in a swarm and group of tremors in a swarm).

**Table 1.1. Number of events causing observations with intensity level at least equal to 6.**

| Event | No. events | No. observations |
|---|---|---|
| Total | 134 | 694 |
| Foreign | 14 | 173 |
| French | 120 | 521 |
| French mainshock | 79 | 342 |
| French foreshock | 1 | 1 |
| French aftershock | 11 | 18 |
| French individual tremor | 15 | 45 |
| French group of tremors | 14 | 115 |

Figure 1.1 shows a subdivision of these events, that can be considered as independent events in the study area, according to the period of occurrence. The first event, for which intensities at least equal to 6 were observed, corresponds to the 23$^{rd}$ of June 1494 earthquake, with epicentre located in the Alps Nicoises. Observation of the figure suggests that the database is very likely

to be incomplete in time. Indeed, an exponential increase with time of the number of events can be observed, but this is not physically realistic, unless it indicates a lack of information on older events, which actually did occur but which are not reported in the catalogue.

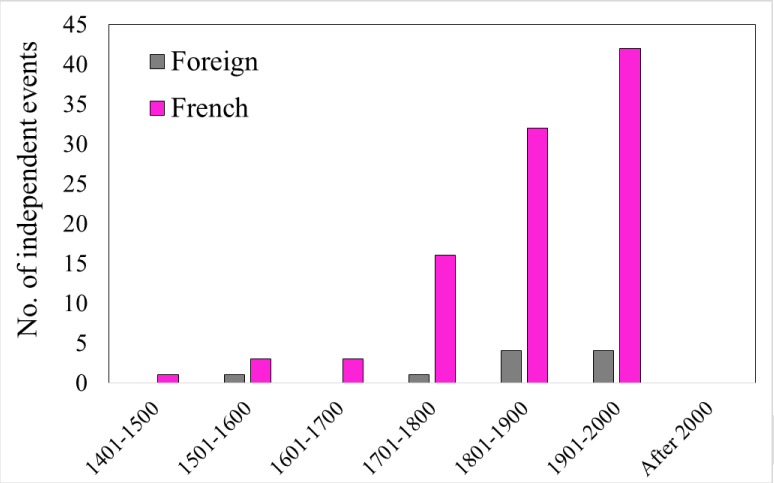


**Figure 1.1. Number of independent events causing observations with intensity at least equal to 6 for different time intervals.**

The statistical analyses carried out on both events and macroseismic observations (for a more detailed description, the reader is referred to Rosti *et al.*, 2014) relative to the study area showed that the available macroseismic data of relevance for the comparison with PSHA results are rather scarce. Indeed, although a very significant number of events is reported in the SisFrance catalogue, with a large number of associated macroseismic observations, the statistical analysis highlighted that only a small percentage of the available macroseismic observations has an intensity level at least equal to 6, corresponding to slight damage on structures according to the MSK scale. All the observations with intensity lower than 6 are therefore, by definition, not associated with any damage to buildings and, hence, when they are transformed into mean damage values, according to the procedure presented in the following of this report, they are very likely to produce null values.

Based on the results obtained from this study of the available database, some critical aspects can be highlighted. First of all, it seems that it could be useful to carry out in-depth macroseismic studies aimed at better characterising events and their associated effects, starting from the strongest ones. Also, some clarifications would be needed on the events classified as swarms. If possible, the completeness in time of the database should be extended by studying historic documentary sources, at least for a restricted area of interest. For engineering purposes, historical information associated with intensity levels below 4 could be removed from the catalogue, as they do not seem meaningful. Moreover, magnitudes of events should be reported.

Results obtained from the statistics on data provided by SisFrance showed that higher macroseismic intensities are mainly due to foreign events. However, as pointed out by Rovida [2013] and Scotti [2013], there are different intensity evaluations between Sisfrance and the databases of neighbouring countries (e.g. the Italian macroseismic database DBMI11, Locati *et*

*al.*, 2011). In particular, it seems that intensity levels attributed by Sisfrance are generally higher than those attributed by other databases. Therefore, further investigations are needed to understand if there is a general bias in the intensity levels provided by Sisfrance or if this issue is only related to foreign events. To this aim, in-depth studies should be carried out in order to homogenise the data related to events occurring at the borders.

## 1.4 Organisation of the report

This work proposes a methodology to compare Probabilistic Seismic Hazard Analyses (PSHA) results with historical information on damage, expressed in the form of macroseismic intensity observations. As mean damage (i.e. the average damage expected in the old building stock) is selected as the metric of the comparison, the first necessary step is the conversion of the values of macroseismic intensity reported in SisFrance into mean damage values. As discussed in Chapter 2, this is done by applying the macroseismic method, proposed by Lagomarsino and Giovinazzi [2006].

The adopted methodology considers different sources of uncertainty, consisting of uncertainty in the historical macroseismic intensity values, in the diffusion of building typologies and in the evaluation of the vulnerability of the different building typologies. All these sources of epistemic uncertainty are taken into account by means of a logic tree approach. The outcome of the logic tree is an equivalent catalogue of mean damage values, each with an associated probability. For each year corresponding to a macroseismic observation, a mean damage value is sampled from the distribution of values derived from the different sources of uncertainty. The rates of exceedance of selected mean damage thresholds are then computed and their statistics are compared with the PSHA results.

Since PSHA results consist of annual probabilities of exceeding different levels of peak ground acceleration (PGA), to allow this comparison, it is required to establish a correspondence between the probability of exceeding the different PGA levels and the probability of exceeding corresponding mean damage levels. The proposed approach is discussed in Chapter 3 and it is based on the use of empirical fragility curves, developed from a large database of post-earthquake damage data collected after the main seismic events occurred in Italy in the last 35 years.

The comparison between observed and expected rates of exceedance of mean damage levels is firstly carried out at individual sites (Chapter 4). However, as metropolitan France is characterised by a relatively low seismicity, the analysis of the database of the available macroseismic observations showed a limited number of events with intensity observations corresponding to structural damage. Due to the limited number and significance of the available macroseismic observations at single sites, it seemed useful to establish a methodology for comparing PSHA results with observations by aggregating multiple sites. The approach adopted for this case is based on the comparison of the empirically-derived and expected (from hazard) mean annual rates of exceedance of preselected mean damage levels. The methodology, tentatively applied to a set of sites, seems to produce encouraging results and allows to counteract the limited information available at individual sites. Based on these considerations, a methodology for the comparison at the regional scale level is presented. The originality of the

proposed method consists in generating a set of spatially correlated random fields of PGA, constrained to the available macroseismic intensity observations. The procedure is then applied to the South-East French territory.

Finally, some preliminary conlcusions on the work carried out are discussed in Chapter 5, with specific attention to the lessons learnt during this project and some suggestions regarding future developments of the work.

# 2 CONVERSION OF MACROSEISMIC INTENSITIES INTO MEAN DAMAGE VALUES

## 2.1 Outline of the proposed methodology

The goal of this study is setting up a methodology for the comparison of PSHA results and macroseismic observations. In order to directly compare empirically-derived rates of exceedances with PSHA results, it is first necessary to identify a metric for the comparison. As in this study the mean damage expected in the building stock is proposed as the selected metric, a procedure for converting macroseismic intensities into mean damage values was derived. The proposed methodology can be articulated into different steps, which are summarised in Figure 2.1 and discussed in the following of this chapter.

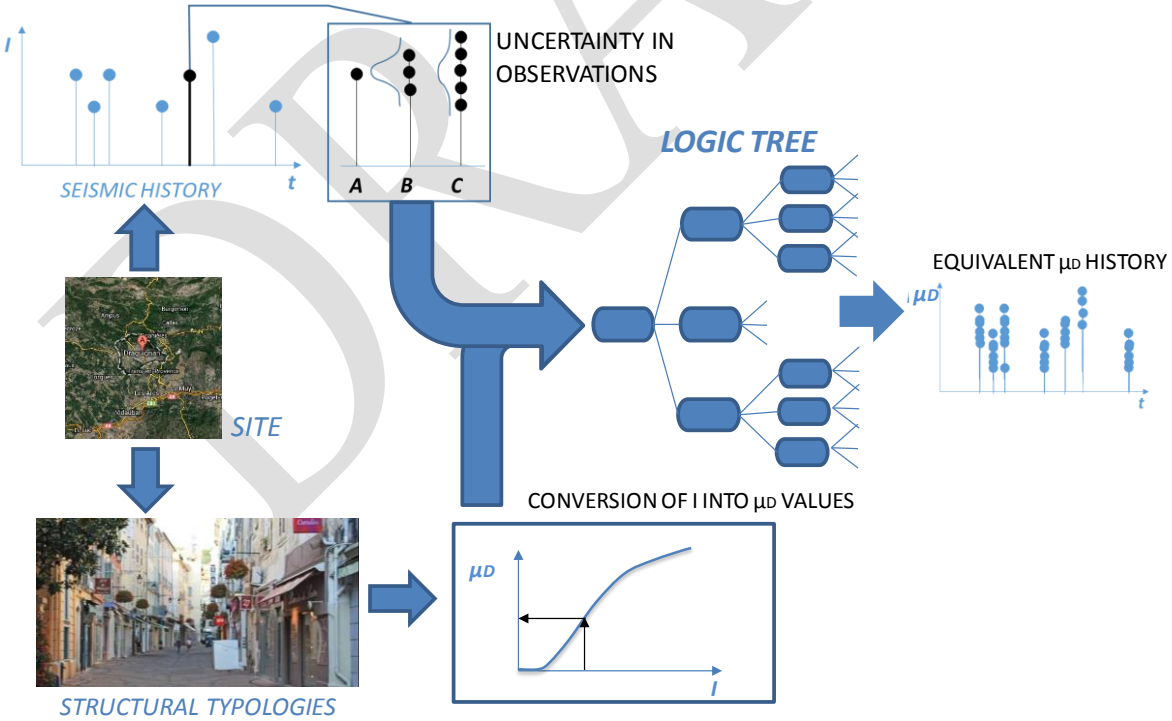


**Figure 2.1. Sketch of the proposed methodology.**

The procedure starts from the selection of a sample of sites with both sufficient macroseismic observations, in terms of number, entity and distribution over time and sufficient information

on the building stock. For each of these sites, the uncertainty on the attributed values of macroseismic intensity (defined by the reliability index reported in SisFrance) is considered, by converting each intensity value into a discrete distribution of values centred on the reported intensity value.

Intensity values then need to be converted into mean damage values by applying the macroseismic method proposed by Lagomarsino and Giovinazzi [2006], which provides an analytical function correlating the expected damage and the macroseismic intensity, as a function of the assessed vulnerability, accounting for the uncertainties in the attribution of the different building typologies to the EMS-98 [Grünthal, 1998] vulnerability classes.

To account for the several sources of uncertainty (i.e. the uncertainty in the reported intensity values, in the building stock and in the attribution of the building typologies to the different EMS-98 vulnerability classes), steps discussed so far are implemented through a logic tree approach, whose outcome is an equivalent mean damage catalogue. Each mean damage value is associated with a date (i.e. the year of the corresponding observed macroseismic intensity) and to a probability, given by the product of the weights of the logic tree branches.

A further optional step was initially considered in the methodology. It consists in the use of spatially correlated random fields for generating synthetic PGA values, in order to integrate the database of available observations for sites for which it is believed to be incomplete. A preliminary analysis of the data reported in SisFrance was presented in Annex 4 of Rosti *et al.* [2014]. The aim was to look for possible discrepancies between the macroseismic intensity observations reported in SisFrance for a given site and the earthquakes which could have been expected to produce a macroseismic observation of intensity at least equal to 6 at the same site. As a further attempt to identify sites for which the seismic history could be integrated with simulated accelerations, the macroseismic intensity data reported in SisFrance for the stronger earthquakes, for which a significant number of observations was available, were plotted to allow for a visual inspection of the distribution of the intensities at least equal to 6. The aim was to identify possible cases of historical gaps, i.e. cases in which the felt intensity was not correctly reported, by identifying the distance within which intensities of at least 6 were reported and possible sites of interest lying within this distance and for which no intensity value was reported in the catalogue.

This preliminary analysis showed that there are no sites with significant possible gaps in the reported values of macroseismic intensity. This means that, at least at this stage of the work and for the sites considered for the presented applications, the application of the random fields for the integration of the available catalogue of observations was not considered further.

## 2.2 Identification of the sites suitable for the comparison

As discussed in detail in the intermediate deliverable of the project [Rosti *et al.*, 2014], the twenty sites for which PSHA hazard curves have been produced within the SIGMA Project were initially considered for a tentative application of the proposed methodology for the comparison of macroseismic observations with the results of PSHA. These sites, shown in Figure 2.2, are located at strategic positions to allow pertinent comparisons either with recorded

accelerometric data or with macroseismic observations. They are sufficiently distant to provide enough independence between the different sites of observations and they cover as homogeneously as possible the whole region of interest.


**Figure 2.2. Map of the South-East quadrant of France, with identification of the twenty sites initially considered.**

For each of these sites, the available macroseismic data were collected and analysed, as discussed in the intermediate deliverable [Rosti *et al.*, 2014]. In particular, the seismic histories, reporting the observed values of macroseismic intensity (in the MSK scale) versus the year corresponding to the seismic event, were declustered by removing foreshocks and aftershocks. Concerning the events classified as "individual tremor in a swarm" and "group of tremors in a swarm", in the case of multiple events occurring in the same year, only the highest local macroseismic intensity level was considered.

Observation of the seismic histories obtained showed that, for most of these initially selected twenty sites, a significant number of macroseismic intensities is less than degree 5 of the MSK scale, i.e. the intensity level for which slight cracks may develop in the plasterwork (very light damage). Hence, a reduced number of sites was considered for applying the proposed methodology, consisting of Grenoble, Valence, Marseille, Nice, Beaumont de Pertuis and Annecy.

By looking at the seismic histories of these sites, it can be observed that Valence is characterised by a limited number of macroseismic observations, all of which are of low intensity levels (no

observations of intensity level at least equal to 6 are available). The seismic history of Marseille and Grenoble shows a higher number of observations, among which only one and two have intensity level at least equal to 6, for Marseille and Grenoble, respectively. The seismic history of Nice is characterised by a significant number of macroseismic intensities exceeding level 5 and it is dominated by a single event significantly stronger than all the others, with an associated macroseismic intensity equal to 8. However, in spite such macroseismic observation is associated with the maximum degree of reliability (A) in the SisFrance catalogue, the same observation is reported in the Italian macroseismic database [Locati *et al*., 2011] with a macroseismic intensity (MCS) equal to 7. Finally, Annecy is the site with the largest number of macroseismic intensity values larger than or equal to 6.

As discussed in Rosti *et al.* [2014], few intensity values of the seismic histories of the sites of interest were reported in SisFrance to be affected by secondary effects, affecting the values of macroseismic intensity. In these cases, the Bayesian updating methodology described in Rosti *et al.* [2014] was used to obtain an estimate of the correct intensity value at the site. This application led to the modification of three values of macroseismic intensity, two of which are in any case very small (5 and 4.5) and hence only have a minor impact in terms of mean damage.

## 2.3 Identification of relevant building typologies and relative diffusion

In order to select the correct fragility curves to be used for the conversion of macroseismic intensities into mean damage values, for each site of study it was necessary to obtain information on the subdivision of the building stock into the different building typologies, with reference to the time of the events for which macroseismic observations are available. All the information collected for this scope for the different sites are reported in Annex 1 of the intermediate deliverable [Rosti *et al.*, 2014]. As the collected information resulted to be very general and not very useful for a precise identification of building typologies at the time of the historical observations, for each site the identification of building typologies was carried out based on expert judgement.

The four building typologies considered to be representative of the historical French building stock are listed in Table 2.1. They all consist of undressed stone masonry buildings with flexible floors, as this is the masonry typology prevailing in the area of study. Minor percentages of adobe and/or timber-framed masonry constructions may be present in some specific sites, but this issue was neglected due to its limited impact and also to the lack of reliable fragility models for these specific construction typologies. Differences among the four considered building typologies concern the number of storeys and the presence or absence of tie-rods and/or tie-beams. In particular, regarding the number of storeys, two classes of height were identified, consisting of buildings with 1-2 storeys and buildings with more than 2 storeys.

Based on the collected information and with the help of expert judgment, different weights (corresponding to the percentage of buildings belonging to a given typology) were associated with each selected building typology, based on the environmental context of each site. As discussed in more detail in Rosti *et al.*, [2014], sites were subdivided into three categories, consisting of larger cities, villages in the Alps and smaller villages. To each of these category, different percentages of the different building typologies were attributed.

**Table 2.1. Selected building typologies for the area of study.**

| | |
|---|---|
| Typology 1 | Undressed stone masonry buildings – flexible floors - with tie rods and/or tie beams and 1-2 storeys |
| Typology 2 | Undressed stone masonry buildings - flexible floors - w/o tie rods and tie beams and 1-2 storeys |
| Typology 3 | Undressed stone masonry buildings - flexible floors - with tie rods and/or tie beams and ≥3 storeys |
| Typology 4 | Undressed stone masonry buildings - flexible floors - w/o tie rods and tie beams and ≥3 storeys |

Among the seven sites considered for the site-specific application of the methodology, Grenoble, Valence, Marseille, Nice and Annecy were assumed to belong to the category of larger cities. Hence, a weight of 0.05 was associated with typology 1, 0.5 with typology 2, 0.15 with typology 3 and 0.30 with typology 4. In the case of Beaumont de Pertuis, belonging to the category of smaller villages, a weight of 0.10 was associated with typology 1, 0.70 with typology 2, 0.05 with typology 3 and 0.15 with typology 4.

## 2.4 Treatment of the uncertainty on the values of macroseismic intensity

The SisFrance database attributes a different code to each macroseismic intensity value, according to the reliability of the information linked to the observation. Code A means that the reported macroseismic intensity is certain, code B corresponds to a fairly certain intensity, whereas code C means that the reported local intensity is uncertain.

To account for this uncertainty, a discrete distribution of intensity values, whose dispersion depends on the reliability of the information linked to the observation, is defined and a weight is attributed to each value. In case of code A, only the macroseismic intensity value reported in Sisfrance is used, with a weight of 1. In case of code B, the reported local intensity value, $I$, and the value $I \pm 0.5$ are considered. In case of code C, the reported macroseismic intensity value, $I$, and the value $I \pm 0.5$ and $I \pm 1$ are considered. For codes B and C, the weight of each intensity value is defined by assuming a normal distribution, centred on the reported intensity value and with a value of standard deviation equal to 0.25 in the case of reliability index B and 0.50 in the case of reliability index C. In particular, the weights are obtained by integrating the area subtended by the normal distribution and bounded by midway percentiles, as shown in Figure 2.3, which reports the two normal distributions used to calculate the weights for reliability index B (left) and C (right). The values obtained for the weights in the different cases are summarised in Table 2.2.

Taking into account the uncertainty associated with the values of intensity reported in the catalogue, the seismic history of a given site is converted into a modified seismic history, in which each intensity value reported in SisFrance is converted into a weighted discrete distribution of intensity values. An example is reported in shown in Figure 2.4, for the case of Nice. The different colours used in the modified seismic history correspond to the weights associated with each single intensity value, as in Figure 2.3. As suggested by Mucciarelli [2014], a non-symmetric intensity distribution could have been alternatively selected.

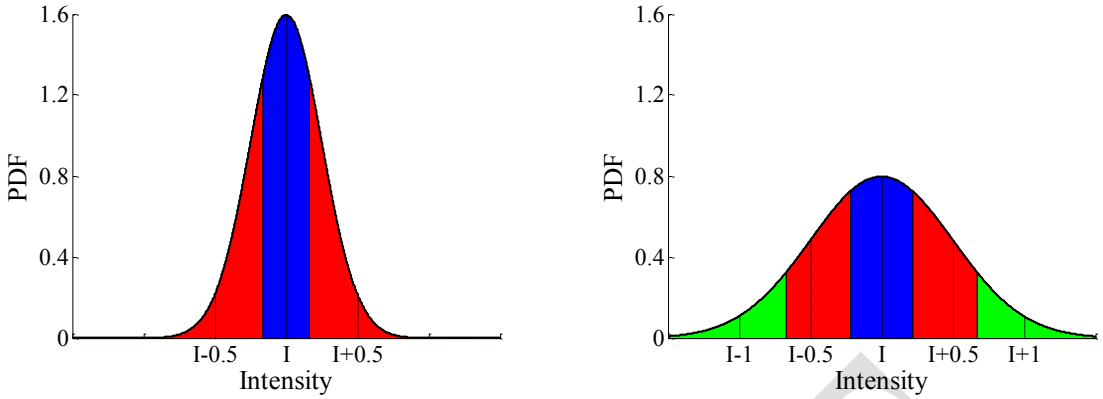


**Figure 2.3. Normal distribution assumed for reliability index B (left) and C (right), used for the calculation of the weights to be attributed to each intensity value.**

**Table 2.2. Weights attributed to each intensity value according to the reliability index of the observation.**

| Intensity level | Code A | Code B | Code C |
|---|---|---|---|
| I-1 | 0 | 0 | 0.09 |
| I-0.5 | 0 | 0.26 | 0.24 |
| I | 1 | 0.48 | 0.34 |
| I+0.5 | 0 | 0.26 | 0.24 |
| I+1 | 0 | 0 | 0.09 |

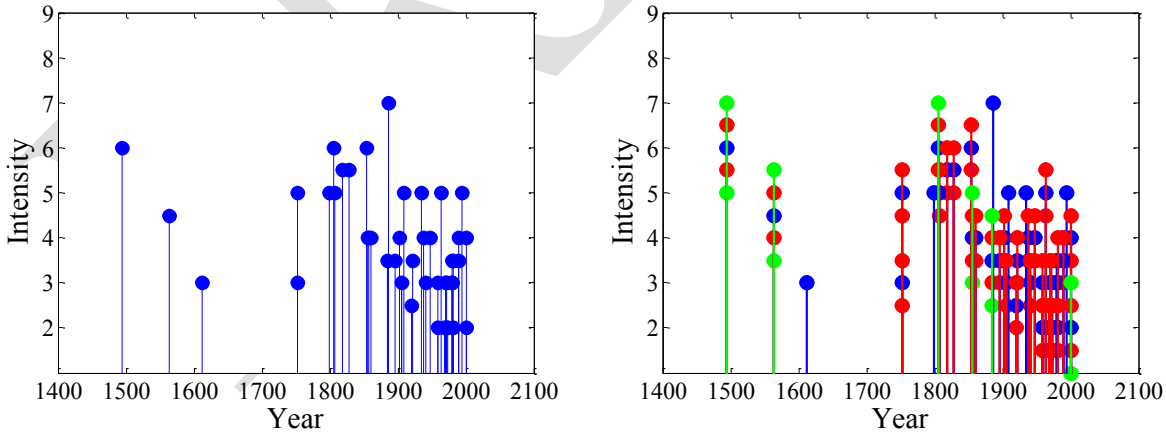


**Figure 2.4. Seismic history of Nice (left) and modified seismic history of Nice taking into account the uncertainty on the macroseismic intensities (right).**

## 2.5 Conversion of intensity values into mean damage values through the macroseismic method

The conversion of macroseismic intensities into mean damage values was carried out by applying the macroseismic method proposed by Lagomarsino and Giovinazzi [2006], which

makes reference to the vulnerability model implicitly included in the definition of the different degrees of the European Macroseismic Scale EMS-98 [Grünthal, 1998]. Both the vulnerability model implicitly defined by the EMS-98 and the macroseismic method are described in more detail in Rosti *et al.*, [2014], but further details can be found in the referenced publications.

In particular, the macroseismic method proposes a closed-form analytical expression correlating mean damage and intensity, as a function of the assessed vulnerability. This expression can be used to compute the mean damage corresponding to a given intensity level, for a selected building typology. Uncertainties in the attribution of the different typologies to the EMS-98 [Grünthal, 1998] vulnerability classes are accounted for by appropriate vulnerability indexes. According to the macroseismic method, for a given building typology, five vulnerability index values are derived from the corresponding membership function through a defuziffication process [Dubois and Prade, 1980], referring to the $\alpha$-cut procedure.

Since the five values of the vulnerability index proposed by Lagomarsino and Giovinazzi [2006] for each building typology do not have any probabilistic significance, in this work they were modified as to correspond to percentiles of the associated membership function (Figure 2.5). In particular, $V$ corresponds to the median of the membership function (50$^{th}$ percentile), $V^{-}$ and $V^{+}$ to the 15.87$^{th}$ and the 84.13$^{th}$ percentiles, whereas $V^{++}$ and $V^{--}$ correspond to the 2.28$^{th}$ and the 97.72$^{th}$ percentiles.

A different weight is then attributed to each vulnerability index value, consistently with the procedure adopted in the case of intensities. As an example, Figure 2.5 shows the computation of these weights for the case of typology 4 (i.e. medium-rise undressed stone masonry buildings without tie-rods and tie-beams). The blue area corresponds to the weight associated with the 50$^{th}$ percentile of the vulnerability index (diamond marker), the red ones are the weights to be attributed to the vulnerability indexes corresponding to the 15.87$^{th}$ and the 84.13$^{th}$ percentiles (dots), whereas the green ones give the weights associated with the vulnerability indexes corresponding to the 2.28$^{th}$ and the 97.72$^{th}$ percentiles (squared markers).

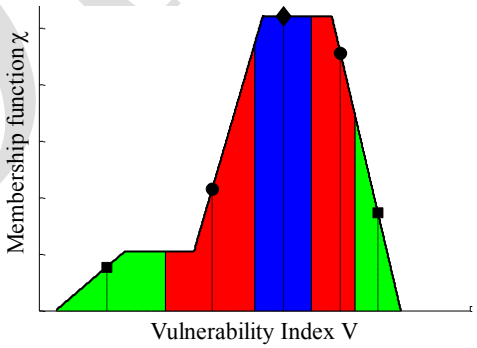


**Figure 2.5. Membership function of medium-rise undressed stone masonry buildings w/o tie-rods and tie-beams (typology 4) and procedure followed for the definition of the weights of the different vulnerability index values.**

The values of vulnerability index obtained for the four selected typologies and the corresponding weights are reported in Table 2.3. Thanks to the procedure used for computing

the weights, they turn out to be equal for corresponding percentiles of the vulnerability index of the different building typologies (Table 2.3).

**Table 2.3. Values of ulnerability index for the four considered building typologies and corresponding weights.**

| Vulnerability index | Typ. 1 | Typ. 2 and 3 | Typ. 4 | Weight |
|---|---|---|---|---|
| $V_{2.28}$ | 0.650 | 0.711 | 0.679 | 0.09 |
| $V_{15.87}$ | 0.686 | 0.773 | 0.801 | 0.24 |
| $V_{50}$ | 0.737 | 0.833 | 0.884 | 0.34 |
| $V_{84.13}$ | 0.794 | 0.870 | 0.950 | 0.24 |
| $V_{97.72}$ | 0.821 | 0.897 | 0.994 | 0.09 |

Once vulnerability index values of each building typology were derived, each intensity level could be converted into five values of mean damage. As an example, Figure 2.6 compares mean damage values for mid-rise undressed stone masonry buildings (left) and for low-rise undressed stone masonry buildings (right). For a given intensity level, the mean damage values are higher in case of mid-rise undressed stone masonry buildings (Figure 2.6, left) and the range of uncertainty of mean damage values is larger with respect to the case of low-rise rubble stone masonry buildings (Figure 2.6, right).

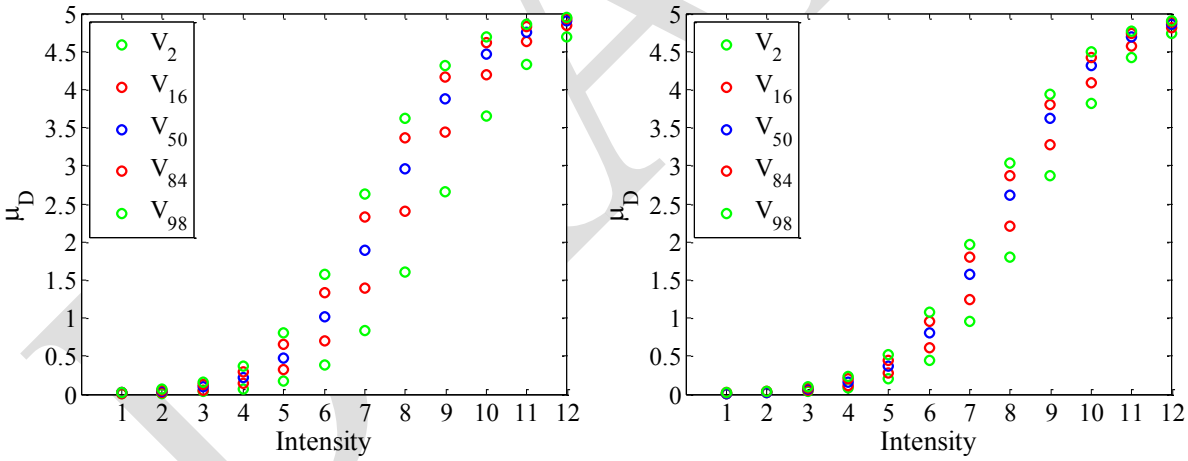


**Figure 2.6. Mean damage values versus intensity levels for mid-rise undressed stone masonry buildings (left) and low-rise undressed stone masonry buildings (right), w/o tie-rods/tie-beams.**

A critical aspect concerning the conversion of intensities into mean damage values is represented by the fact that macroseismic intensities can be expressed by different scales. In Sisfrance, macroseismic intensities are expressed according to the MSK scale [Medvedev *et al.*, 1964], whereas the macroseismic method refers to the EMS-98 scale [Grünthal, 1998]. In this work, it has been assumed that the mean values of each intensity class can be considered equivalent in the two macroseismic scales, consistently with literature studies [e.g. Musson *et al.*, 2010], whereas the uncertainty in the estimate of the intensity values is explicitly considered.

## 2.6 Derivation of the equivalent mean damage catalogue

To account for the different sources of uncertainty (i.e. uncertainty in the reported intensity values, in the building stock and in the attribution of the building typologies to the different EMS-98 vulnerability classes), the steps discussed so far are implemented through a logic tree approach, according to the scheme reported in Figure 2.7.

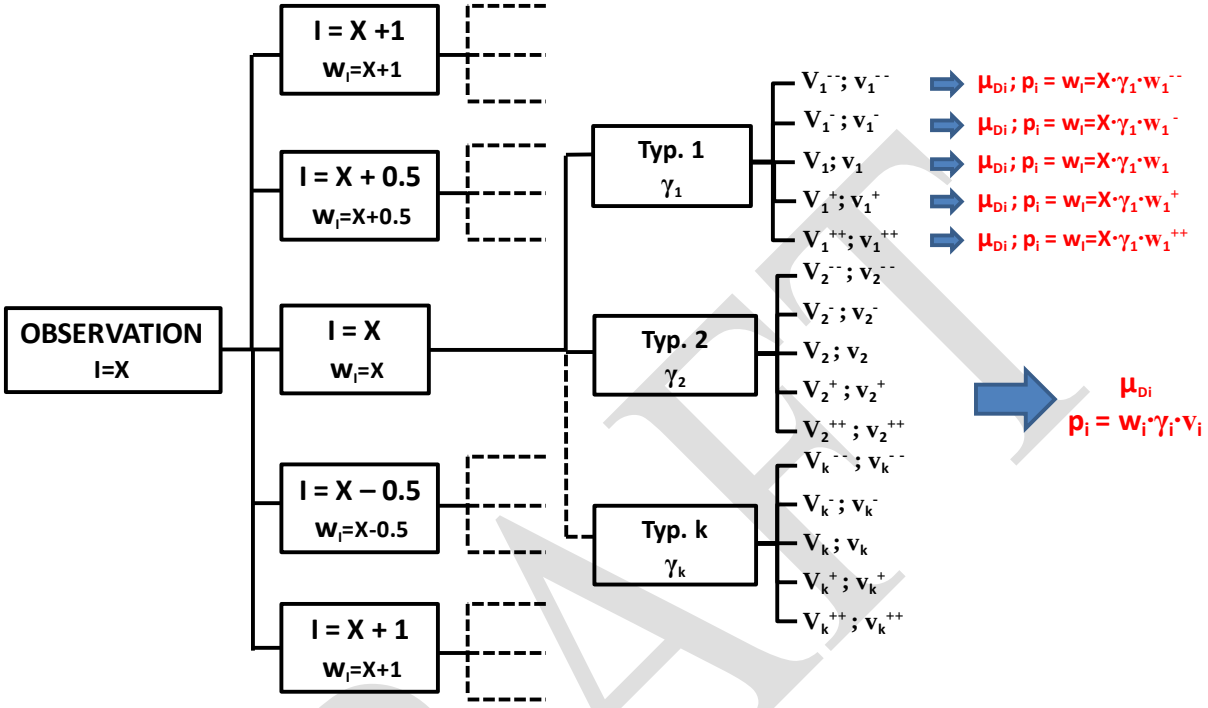


**Figure 2.7. Logic tree approach proposed in the methodology.**

The application of the procedure to each observed macroseismic intensity of the SisFrance catalogue allows to obtain an equivalent mean damage history, in which each mean damage value is associated to a date (i.e. the year of the corresponding observed macroseismic intensity) and to a probability, given by the product of the weights of the logic tree branches.

Figure 2.8 shows an example of application of the logic tree procedure through which the intensity seismic history of a generic site is transformed into an equivalent mean damage history. At the top left of the figure, the seismic history of a site of interest is shown, taking into account only macroseismic intensities related with mainshocks. The top right part of the figure shows the modified seismic history of the same site, accounting for the reliability index associated with each observed intensity, with colours corresponding to the weights associated with each single intensity value. Finally, the bottom part of the figure reports the equivalent seismic history in terms of mean damage values, given by the outcomes of the logic tree.

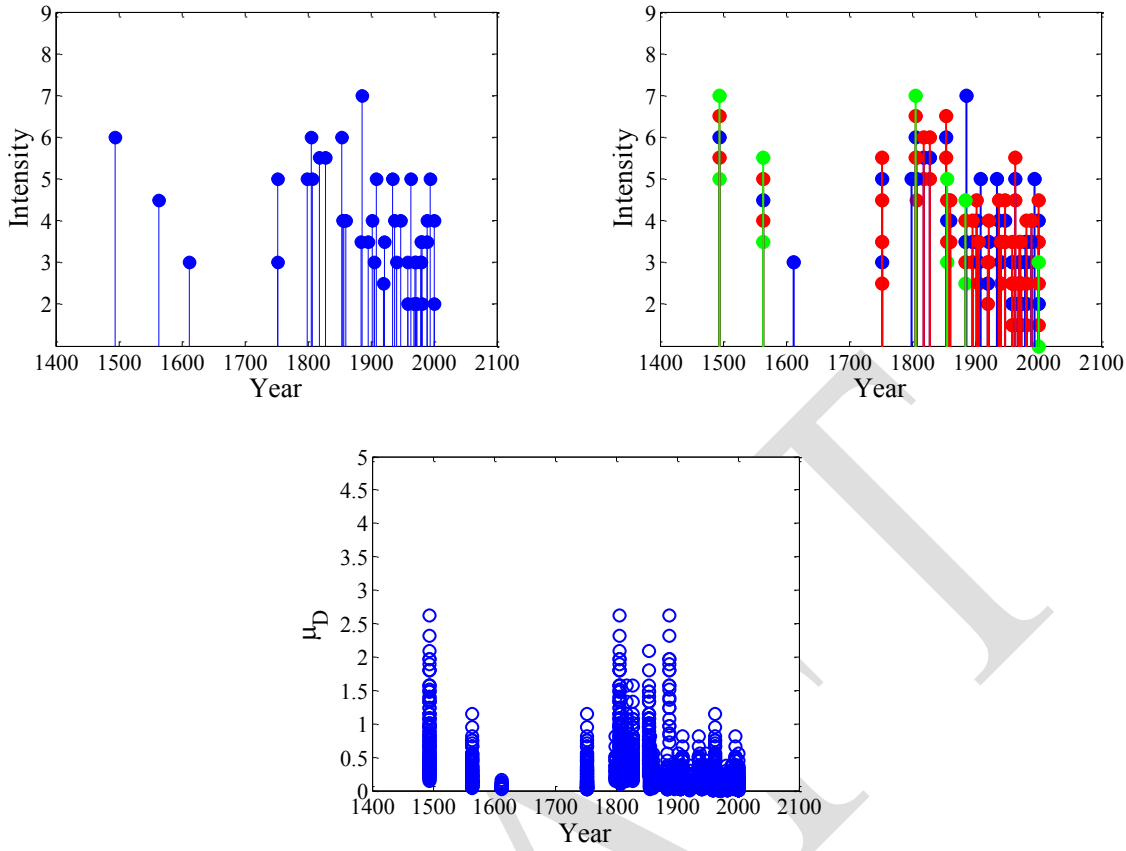


**Figure 2.8. Seismic history of a generic site in terms of macroseismic intensities (top left); modified seismic history accounting for uncertainty in the macroseismic intensities (top right); seismic history in terms of mean damage accounting for all the sources of uncertainty (bottom).**

## 2.7 Annual rates of exceedance of mean damage thresholds

As previously explained, the outcome of the logic tree approach is an equivalent catalogue in terms of mean damage values, each with its associated weight. The set of mean damage values accounts for all the sources of uncertainty as it derives from consideration of uncertainties in macroseismic intensities, building typologies and attribution of the different typologies to the EMS-98 vulnerability classes.

A Monte Carlo approach is then used to sample mean damage values from the equivalent catalogue resulting from the implementation of the logic tree, in order to obtain, at each run, one single value of $\mu_D$ for each year in which a macroseismic observation is available. An example of this operation is shown in Figure 2.9, which shows the equivalent catalogue in terms of mean damage for a given site (on the left) and the seismic histories obtained at two generic Monte Carlo runs (on the right).

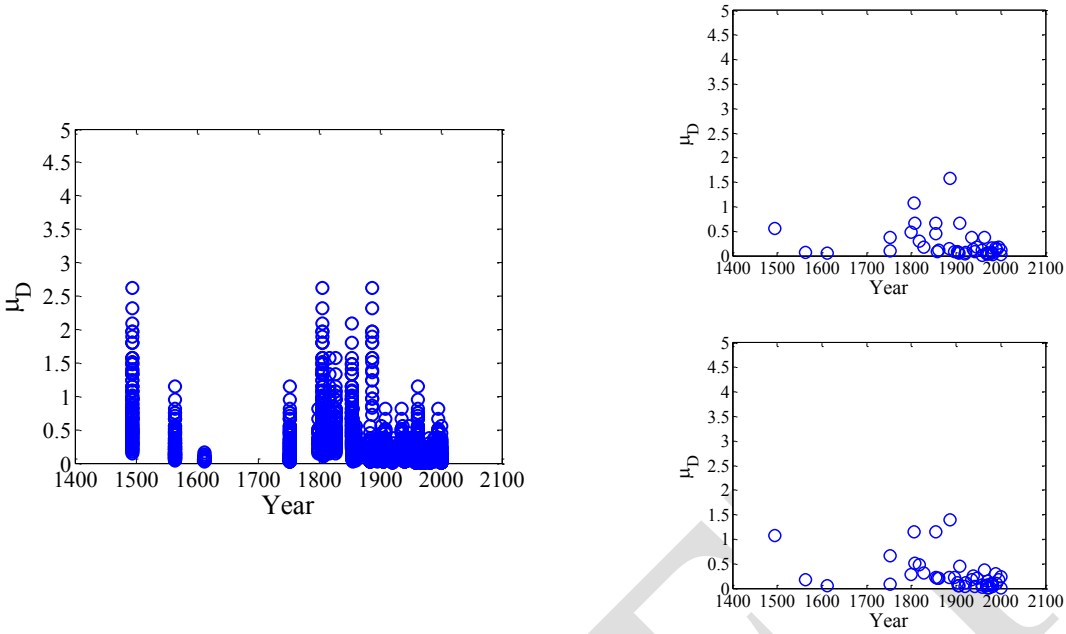


**Figure 2.9. Equivalent catalogue in terms of mean damage for a given site (left) and seismic histories obtained from two generic Monte Carlo runs (right).**

Based on the results of this extraction, at each run and for each predefined mean damage level, the observation period and the best estimate of the annual rate of exceedance (i.e. number of exceedances of the selected mean damage level over the corresponding observation period) are computed. In particular, the observation period is evaluated as the difference between the last year for which SisFrance provides observations (i.e. 2007) and the first year in which a $\mu_D$ value lower than or equal to the selected level is observed. This implicitly assumes that, starting from the year in which a given value of intensity is reported, the seismic history of the site is complete for all $\mu_D$ levels equal to or higher than the reported value. On the contrary, the catalogue cannot be assumed to be complete for lower $\mu_D$ levels. It should be noted that, using this definition, the observation period of each $\mu_D$ level varies from run to run, as the sampled values of $\mu_D$ vary as well.

The best estimate of the rate of exceedance of the considered $\mu_D$ threshold is then given by the ratio of the number of times the $\mu_D$ level is exceeded and the observation period. Also, the 90% confidence bounds of the population proportion (i.e. number of exceedances over the number of observations in the observation period) are determined, under the assumption of binomial distribution, whose limits of validity were discussed in Rosti *et al.* [2014]. These confidence limits are then converted into bounds of the best estimate of the empirically-derived rates of exceedance.

Since Monte Carlo approach is repeated several times, statistics of the best estimate of the empirically-derived rates of exceedance and of its 90% confidence bounds are computed. These quantities will be compared with the corresponding results obtained from PSHA predictions, as discussed in a following section.

# 3 CONVERSION OF PGAS INTO MEAN DAMAGE VALUES

## 3.1 Outline of the proposed methodology

PSHA results are expressed in terms of rates of exceedance of PGA levels. To allow the comparison with historical observations, these rates of exceedance of PGAs obtained from PSHA studies need to be connected to mean damage values.

In this work, PGAs are converted into mean damage values by means of fragility curves. As discussed in more detail in the following section, taking advantage of the similarity between the South-East French and Italian building stock, empirical fragility curves derived from the statistical elaboration of post-earthquake damage data gathered after Italian earthquakes (in the period 1980-2009) are used for the conversion. The integrated dataset includes approximately 150000 buildings and allows the derivation of fragility curves in the PGA range from 0 to 0.5g.

For each selected building typology, the probabilities of reaching different damage levels are computed from the corresponding fragility curves and a mean damage curve is then obtained, as discussed in a following section. This curve allows to establish a relationship between a given level of PGA and the corresponding mean damage value, for a given building typology.

The combination of the mean damage versus PGA curves derived for the different building typologies of interest allows to obtain a value of mean damage for each level of PGA and, hence, to associate PSHA rates of exceedance to mean damage levels.

## 3.2 Fragility curves

The reasons behind the choice of using empirical fragility curves derived from Italian post-earthquake damage data were already discussed in some detail in Rosti *et al.* [2014]. Basically, this choice was based on the assumed similarity between the building typologies typical of the South-East French historical building stock and some of the typologies for which Italian post-earthquake damage data are available. This assumption was also confirmed by the investigations carried out on the selected sites, which are reported in Annex 1 of Rosti *et al.* [2014]. Moreover, the use of empirical fragility curves calibrated independently from the French historical macroseismic data was deemed necessary for the implementation of an unbiased comparison.

The fragility curves proposed by Rota *et al.*, [2008a, b] and discussed in Rosti *et al.* [2014] were further improved by integrating survey data gathered after the event of L'Aquila (2009).

After processing of the available data and considerations on survey completeness, the database finally used for the derivation of fragility curves includes 142259 usable data, among which 58408 correspond to the four undressed stone masonry building typologies of interest for this study.

The main aspects related to the derivation of the empirical fragility curves used in this study are briefly discussed in the following.

### *3.2.1 Adopted integrated database of post-earthquake damage data*

As already mentioned, post-earthquake survey data collected after several Italian earthquakes (1980-2002) and processed by Rota *et al.* [2008a, b], were integrated by L'Aquila (2009) damage data. The purpose was essentially to create an updated database allowing an improvement of the available empirical data thanks to the addition of a significant number of data at higher PGA levels. The seismic events considered for the creation of the integrated database are listed in Table 3.1. Data were retrieved from the parametric catalogue of Italian earthquakes.

**Table 3.1. Main characteristics of the considered earthquakes – from the parametric catalogue of Italian earthquakes.**

| Earthquake | Year | Epicentre | | M |
|---|---|---|---|---|
| | | Latitude | Longitude | |
| Irpinia | 1980 | 40.85 | 15.28 | 6.89 |
| Abruzzo | 1984 | 41.666 | 14.057 | 5.67 |
| Umbria-Marche | 1997 | 43.019 | 12.879 | 5.95 |
| Pollino | 1998 | 40.038 | 15.937 | 5.35 |
| Molise | 2002 | 41.694 | 14.925 | 5.59 |
| L'Aquila | 2009 | 42.34 | 13.38 | 6.1 |

The data collected after the different events were homogenised, by subdividing them into a number of building typologies and damage levels. This operation required some assumptions, as the survey forms used for post-earthquake damage data collection evolved with time. All the hypotheses and criteria used in this phase of the work are discussed in detail in Rota *et al.* [2008a, b].

As discussed in more detail elsewhere, buildings were subdivided into 23 typologies, on the basis of the type of vertical structure, the number of storeys, the period of construction (in relation with the enforcement of seismic design regulations) and, for the case of masonry buildings, the masonry layout, the in-plane flexibility of the horizontal structure and the presence of aseismic devices (tie rods and/or tie beams). As already discussed (section 2.3), only four building typologies were considered as relevant for the South-East France, all consisting of undressed stone masonry buildings with flexible floors (Table 2.1).

The derivation of empirical fragility curves also requires the selection of a parameter able to accurately represent the ground motion. In this work, PGA was selected for representing the ground motion. In particular, a single value of PGA, evaluated by means of an attenuation law, was attributed to each municipality affected by one of the considered earthquakes. The reasons of these choices and the assumptions used are discussed in detail in Rota *et al.* [2008b].

Consistently with the European Macroseismic Scale, five damage grades plus the absence of damage, DS0, were considered: negligible to slight damage (DS1), moderate damage (DS2), substantial to heavy damage (DS3), very heavy damage (DS4) and destruction (DS5). The hypotheses used for converting all the damage scales included in the various post-earthquake survey forms into this unique scale are reported elsewhere [Rota *et al.* 2008].

In order to derive the finally used version of the database, it was also necessary to take into consideration the issue of survey completeness, in order to obtain an unbiased sample of data. To this aim, a percentage of completeness of 60% was selected, in accordance with Rota *et al.* [2008a, b].

The integrated dataset obtained after this elaboration of the available data hence includes 142259 usable data (after the removal of constructions with non-identified damage level).

Figure 3.1 shows the subdivision of tahe data of the entire database (142259 building data, referring to the 23 typologies considered by Rota *et al.*, 2008a) based on the type of vertical structure and the contribution of each earthquake in terms of number of buildings.

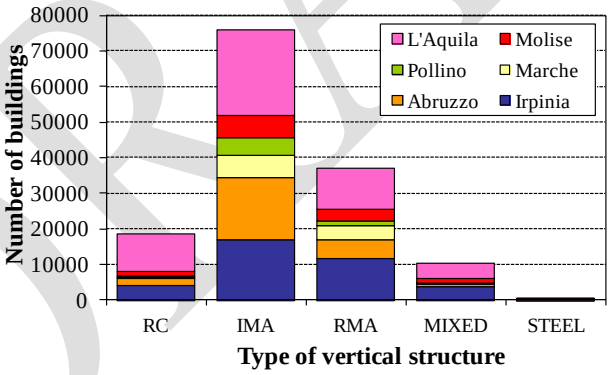


**Figure 3.1. Number of buildings as a function of the type of vertical structure and the origin of the data, referring to the entire database of 142259 data.**

Figure 3.2 refers instead only to the four building typologies of interest for the area of study and, in particular, it shows the subdivision of the (58408) data into the four building typologies (left) and into the different PGA intervals (right).

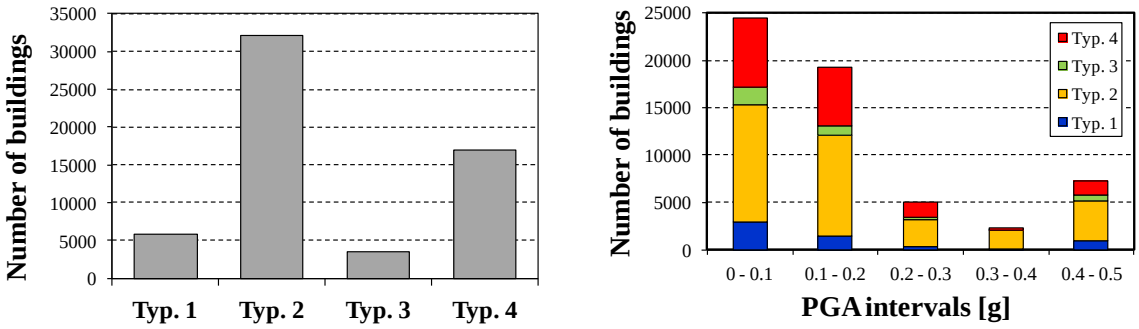


**Figure 3.2. Number of buildings belonging to the four considered building typologies (left) and to the different PGA levels (right).**

### *3.2.2 Derivation of fragility curves and considerations on the results obtained*

The derivation of the empirical fragility curves used in this study required the following steps:

- Determination of the Damage Probability Matrixes (DPMs), representing, for each building typology and for each PGA interval, the experimental probability of occurrence of the different damage states.

- Computation of the probability of exceeding a certain damage state by cumulating the experimental frequencies from the highest to the lowest level of damage.

- Fitting of the experimental data with a lognormal cumulative distribution by means of the nonlinear regression algorithm of Levenberg and Marquardt [Levenberg 1944; Marquardt, 1963].

Observation of the DPMs showed that, for some typologies, the presence of pre-existing damage is extremely evident, as shown by the large predominance of DS1 over the other damage state probabilities, independently from the level of ground motion. Moreover, the fragility curve obtained for damage level DS1 for some building typologies showed a peculiar shape, characterised by an initial steep branch with a subsequent flat trend. This shape seems to be governed by the first experimental point (i.e. data corresponding to a PGA value of 0.025g), which indicates an unrealistically high percentage of buildings (as high as 90% for the case of typology 1) having suffered damage level DS1 for PGAs lower than 0.05g. This trend may be justified by the presence of pre-existing damage, which is typical of masonry buildings and is likely to be of modest entity and hence it affects mainly the empirical data for DS1 (and potentially the following damage states resulting from worsening of a pre-existing slight damage). Another possible reason can be related to the issue of survey completeness, which leads to an underestimation of the percentage of undamaged buildings, particularly in the areas further away from the epicentre, which are hence characterised by low values of ground motion.

Based on these considerations, the obtained fragility curves were modified, by ignoring the experimental points in the first PGA interval (i.e. PGA = 0.025g). The so obtained modified empirical fragility curves for the four considered building typologies are shown in Figure 3.3. These are the fragility curves that were adopted in the following of this study.

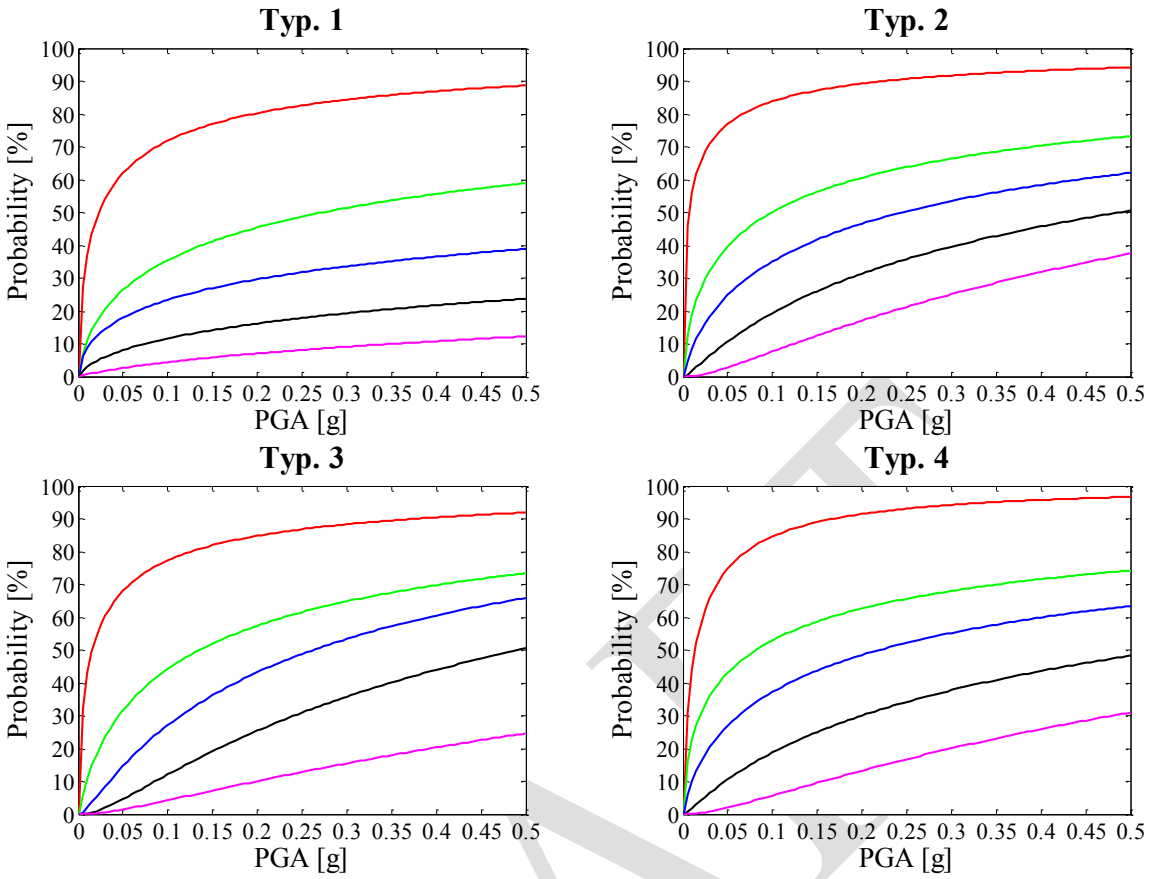


**Figure 3.3. Modified empirical fragility curves for the four considered building typologies.**

Despite the introduced modification, the obtained modified empirical fragility curves still show a trend which is not the typical lognormal shape, indicating that probably the distribution of the empirical data into the different damage and PGA levels does not follow a lognormal model. Alternative models could be hence explored, trying to improve the fitting of the empirical data. Also, despite the removal of the first empirical point (lowest PGA level), the role of the endemic damage still appears to be significant. This aspect could be further explored.

## 3.3 Derivation of the mean damage versus PGA curve

For each considered building typology, the probabilities of reaching different damage levels are computed from the corresponding fragility curves. Under the assumption of a binomial distribution of damage between the different damage grades, a commonly accepted assumption [e.g. Braga *et al.*, 1982; Lagomarsino and Giovinazzi, 2006], the mean damage curve is obtained, as a function of PGA, for each building typology, according to:

$$\mu_d = \sum_{k=0}^{5} p_k k \tag{3.1}$$

where $p_k$ represents the probability of having damage grade $D_k$ ($k$ = 0÷5). An example is reported in Figure 3.4 with reference to building typology 1.

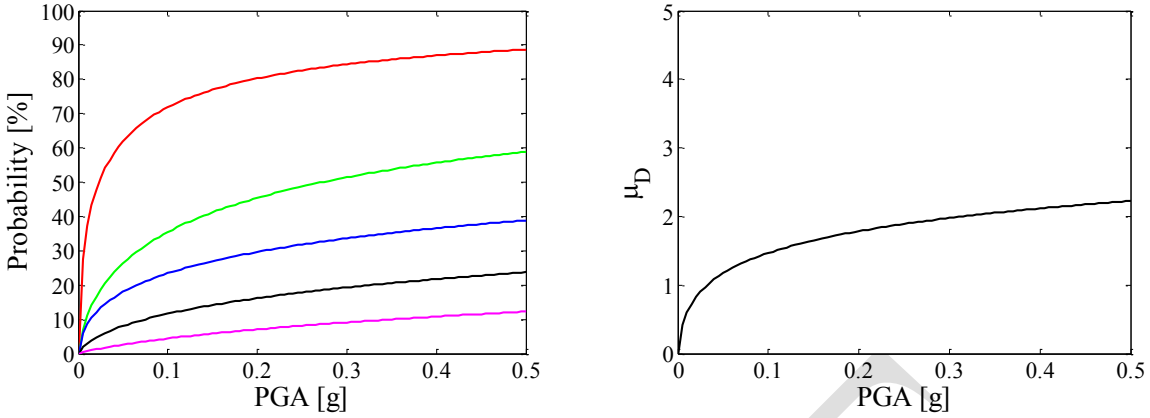


**Figure 3.4. Fragility curves obtained for building typology 1, for the different damage levels (left) and mean damage curve obtained by applying Equation 3.1 (right).**

Given a PGA level, a value of mean damage can then be derived from the PGA-$\mu_D$ curve of each building typology. This step is repeated for each selected building typology providing, for a given PGA threshold as many mean damage values as the selected building typologies are. A single value of mean damage is then derived as the weighted average of the different values. The conversion of PGA thresholds into mean damage values hence allows to define a single mean damage versus PGA curve (Figure 3.5, top right plot), which will be used to associate PSHA rates of exceedance to mean damage levels, as discussed in the following section.

## 3.4 Conversion of PSHA rates of exceedance of PGAs into probability of exceedance of mean damage value

The results of PSHA are provided in the form of curves, representing the probability of exceedance of different PGA levels. Curves are obtained from the elaboration of the results of a logic tree, accounting for the epistemic uncertainty in the definition of seismic hazard. For this reason, different curves are provided for each site, corresponding to different percentiles of the results of the PSHA logic tree.

In order to allow comparison with the mean damage rates of exceedance derived from macroseismic observations, it was hence necessary to convert the PGA levels, for which PSHA results provide values of the probability of exceedance, into mean damage levels. This was done with reference to the mean damage versus PGA curve obtained by combining the corresponding curves for the considered building typologies, as discussed in the previous section.

This operation is sketched in Figure 3.5. In particular, the top left plot shows the hazard curves provided for a generic site, corresponding to the median (50$^{th}$ percentile), the 5$^{th}$, 16$^{th}$, 84$^{th}$ and 95$^{th}$ percentiles of the PSHA results. The top right plot shows the mean damage curve, as a function of PGA, obtained as a weighted combination of the curves for the four considered building typologies. Finally, the bottom plot shows the curves connecting PSHA rates of exceedance to mean damage levels and hence providing the rates of exceedance of mean damage values that can be compared with the equivalent quantities derived from historical observations.

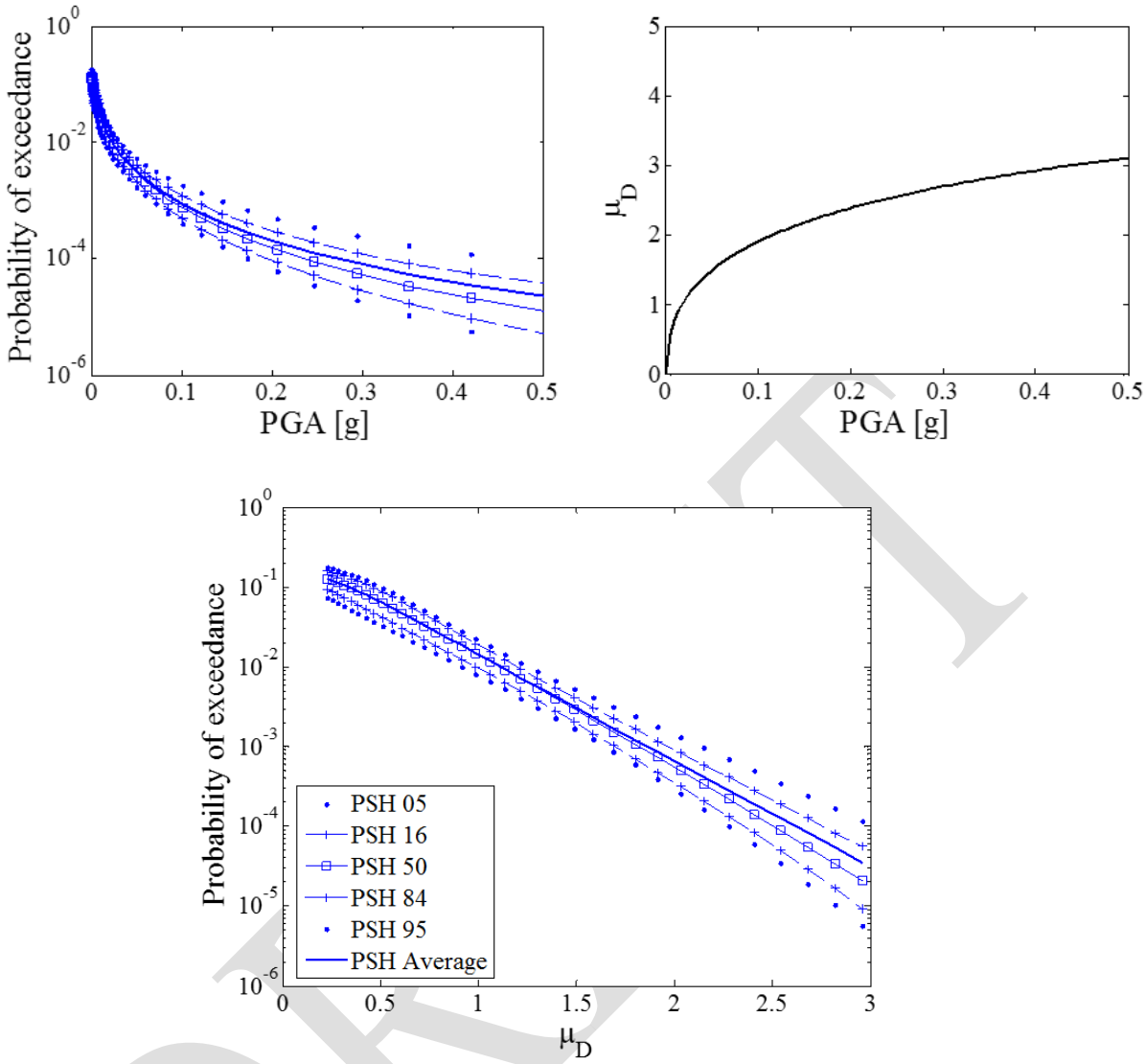


**Figure 3.5. PSH hazard curves for a generic site (top left); mean damage curve versus PGA (top right) and curves expressing PSHA rates of exceedance of mean damage levels (bottom).**

# 4 PROPOSED METHODOLOGIES FOR COMPARING PSH RESULTS AND HISTORICAL OBSERVATIONS AT DIFFERENT SCALES

## 4.1 Introduction

This Chapter presents three different approaches for comparing PSH results with information from historical observations. The scale level at which each comparison is carried out represents the main feature distinguishing the proposed methods. A procedure for site-specific comparison is first outlined and examples of application are also provided (Section 4.2). As an alternative, the comparison of PSH results with historical observations can be performed by aggregating information available at different sites (Section 4.3). In this case, sites are aggregated one to each other and treated as a single one. Sampling in space allows to make up for the limited availability of macroseismic data at individual sites, suggesting the opportunity of developing a method for the comparison at a larger scale level. The methodology is hence applied to a set of sites, located within the study area. The interesting results obtained for aggregated sites suggested to develop a procedure for the comparison at the regional scale, starting from the method originally proposed by Labbé [2010]. The proposed methodology is presented in Section 4.4 and is then applied to the South-East French territory.

## 4.2 Site-specific comparison

A methodology for comparing PSH results with observations at individual sites is first presented. The comparison is intended to be performed in terms of annual rates of exceedance of preselected mean damage thresholds. Site-specific comparisons may be very useful for sites of particular interest, such as nuclear installations sites, for which having an immediate comparison of PSH predictions with historical data could be worthwhile. Nonetheless, site-specific comparisons are unavoidably affected by the seismic history of the selected sites. In this sense, the limited number of macroseismic data of engineering interest may represent a shortcoming, preventing pertinent comparisons with PSH results. In the following, two examples of application of the methodology are provided in order to point out strengths and weaknesses of such a procedure. To this purpose, the site of Annecy was first selected, as it is one of the sites of interest with the most significant seismic history, both in terms of number and entity of the observations. On the other hand, the methodology is then applied to Marseille,

which is a site with a more limited amount and significance of observations, in order to show how the lack of macroseismic data of engineering interest can impact the results.

### *4.2.1 Annecy*

Annecy represents a good candidate for the application of the procedure. Indeed, with respect to the other sites, its seismic history shows a significant number of macroseismic observations exceeding intensity level 5 (Figure 4.1, left). To account for the different reliability levels of the observations, each observed macroseismic intensity is then converted into a weighted distribution of intensity values (Figure 4.1, middle). Based on the environmental context of the site (i.e. larger city), weights equal to 0.05, 0.50, 0.15 and 0.30 are attributed to the identified building typologies (Table 2.1). By applying the macroseismic method to each macroseismic intensity and considering each building typology, an equivalent seismic history in terms of mean damage is obtained (Figure 4.1, right). It is noted that a weighted distribution of mean damage values is associated with each year corresponding to a macroseismic observation.

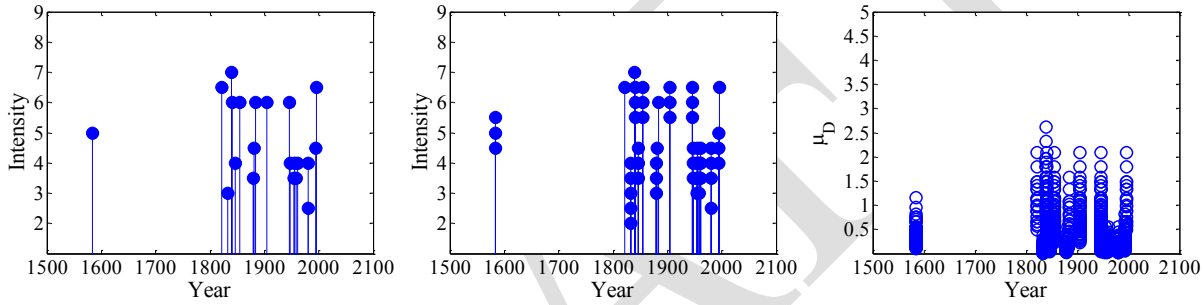


**Figure 4.1. Seismic history (left), seismic history accounting for uncertainty in the macroseismic intensities (middle), equivalent mean damage history (right) of Annecy.**

On the other side, PGA levels, for which PSH estimates are provided, need to be converted into mean damage values to allow the comparison. As previously explained, such conversion is performed by using the empirical fragility curves corresponding to each selected structural typology, so that a mean damage curve as a function of PGA is derived. Since a mean damage value is associated with a PGA threshold, each mean damage value, corresponding to a PGA threshold, can be then easily associated with PSH rates of exceedance, provided for different percentiles. These steps are sketched in Figure 4.2.

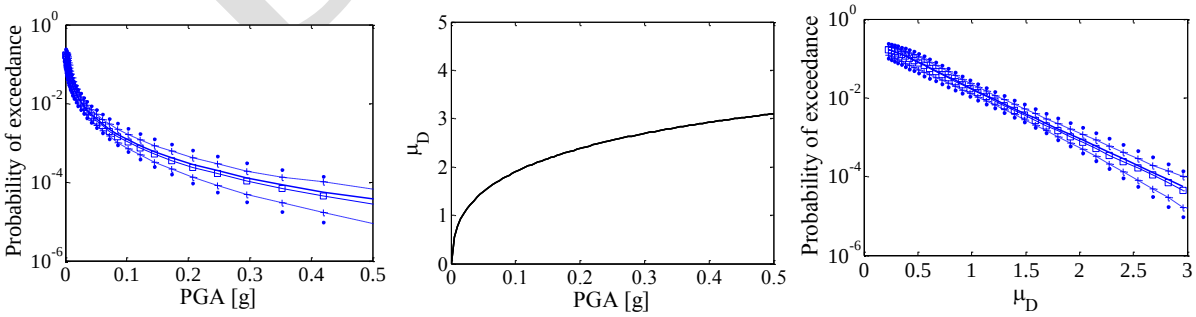


**Figure 4.2. PSHA curves of different percentiles (left), mean damage curve as a function of PGA (middle), rates of exceedance of mean damage levels (right), for the site of Annecy.**

On the left, PSH predictions for Annecy, corresponding to different percentiles, are shown. In the middle, the mean damage curve as a function of PGA, obtained by combining the empirical fragility curves, is depicted, whilst PSH rates of exceedance of mean damage levels are shown on the right.

Empirically-derived rates of exceedance of preselected mean damage levels are then plotted against PSH estimates (Figure 4.3). In this application, ten mean damage thresholds, ranging from 0.5 to 2.75, with an increment of 0.25, are considered. In the figure, red corresponds to the best estimate of the empirically-derived rates of exceedance, whilst the upper and lower 90% confidence bounds are in black and green, respectively. Diamonds correspond to the average, circles to the median, whilst the error bars represent the variability within the several Monte Carlo runs (i.e. 5$^{th}$ and 95$^{th}$ percentiles).

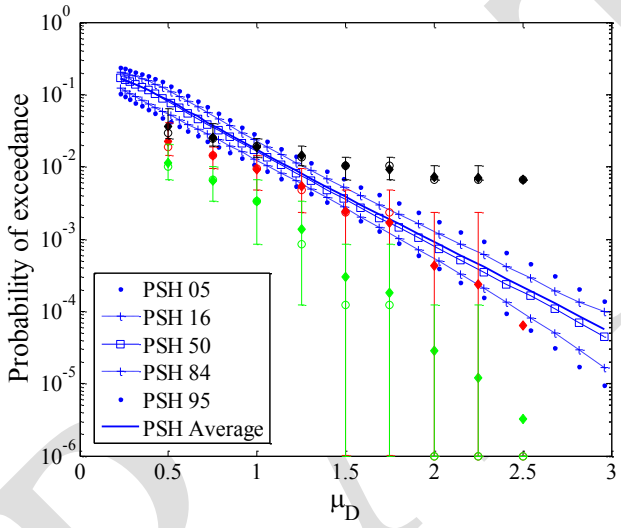


**Figure 4.3. Comparison of PSH predictions of different percentiles with meaningful statistics of the best-estimate (red) and of the upper (black) and lower (green) 90% confidence limits of the empirically-derived annual rates of exceedance of predefined mean damage levels (Annecy). Diamonds: average; circles: median; error bars: 5$^{th}$ and 95$^{th}$ percentiles.**

It can be noted that, starting from a mean damage level equal to 1, PSH results are consistent with the best estimate of the empirically-derived rates of exceedance. At the lower mean damage levels, instead, PSH estimates tend to overestimate results from historical observations. This could be explained by the fact that some low intensity macroseismic observations may not be reported in the historical catalogue. It is also observed that smaller uncertainties on the best-estimate correspond to lower mean damage thresholds, whilst they increase at higher mean damage levels. Indeed, the significant number of low mean damage values, characterising the equivalent mean damage history, allows to reach higher confidence in the empirically-derived rates of exceedance at the lower levels of mean damage.

### *4.2.2 Marseille*

Site-specific comparison is here applied to the site of Marseille, in order to show how the small entity of observations characterising the seismic history of many sites in the area of interest may not allow to obtain meaningful results to be compared with PSH predictions. The seismic

history of Marseille (Figure 4.4, left) shows indeed a rather significant number of observations, but they are all characterised by low intensity levels (there is only one observation of intensity level 6 and all the others are lower than 6). Based on the environmental context of site (i.e. larger city), weights equal to 0.05, 0.50, 0.15 and 0.30 were attributed to the four selected structural typologies (Table 2.1). Figure 4.4 (middle) shows the seismic history accounting for uncertainty in the intensity levels. On the right, the equivalent mean damage history, resulting from the implementation of the logic tree approach, is depicted. It is observed that very low mean damage values characterise the equivalent mean damage history.

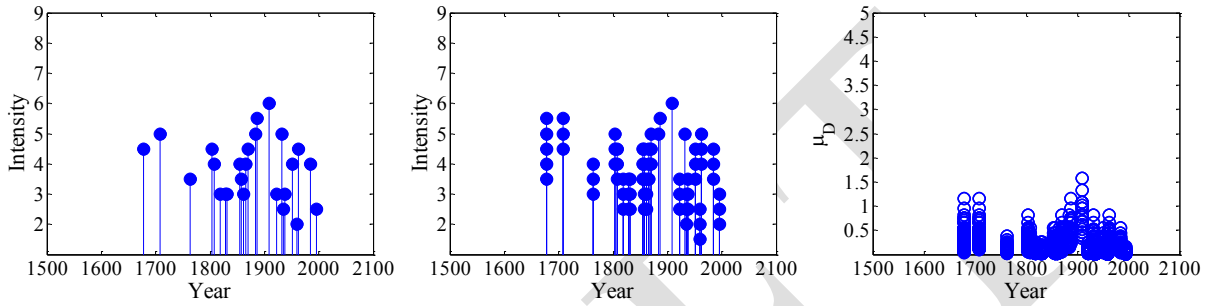


**Figure 4.4. Seismic history (left), seismic history accounting for the uncertainty in the macroseismic intensities (middle), equivalent mean damage history (right) of Marseille.**

Figure 4.5 shows the PSH rates of exceedance for different percentiles (left), the mean damage curve resulting from the combination of the selected fragility curves (middle) and the PSH rates of exceedance of mean damage levels.

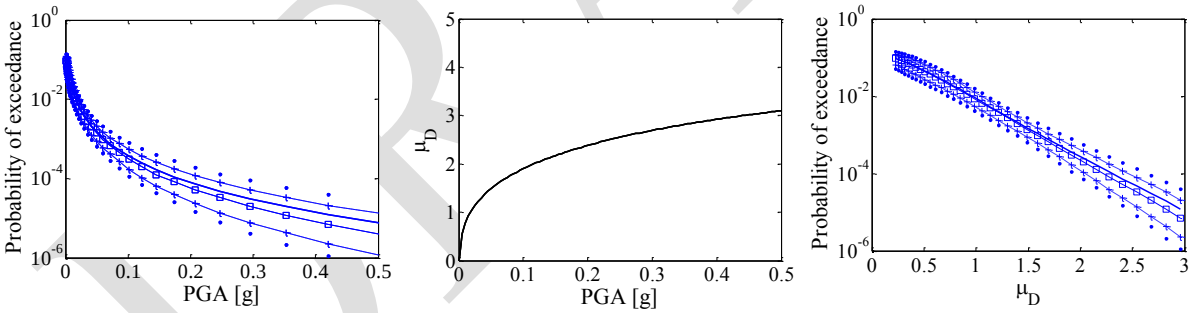


**Figure 4.5. PSHA curves of different percentiles (left), mean damage curve as a function of PGA (middle), rates of exceedance of mean damage levels (right), for the site of Marseille.**

Figure 4.6 compares meaningful statistics of the empirically-derived annual rates of exceedance of the preselected mean damage thresholds with PSH estimates. In the figure, red refers to the best-estimate of the empirically-derived rates of exceedance, black and green to the upper and lower 90% confidence bounds, respectively. Diamonds correspond to the average whilst circles to the median. The error bars, accounting for the variability over the several Monte Carlo runs, correspond to the 5$^{th}$ and 95$^{th}$ percentiles. It is observed that the low entity of macroseismic observations prevents pertinent comparison with PSH estimates. Indeed, rates of exceedance from observations are available only for a very limited range of mean damage values. Moreover, very large uncertainty on the best estimate is observed, even at the lowest mean damage levels. This is essentially due to the large number of mean damage values falling below the first

selected mean damage threshold and hence determining the low confidence in the empirical results.

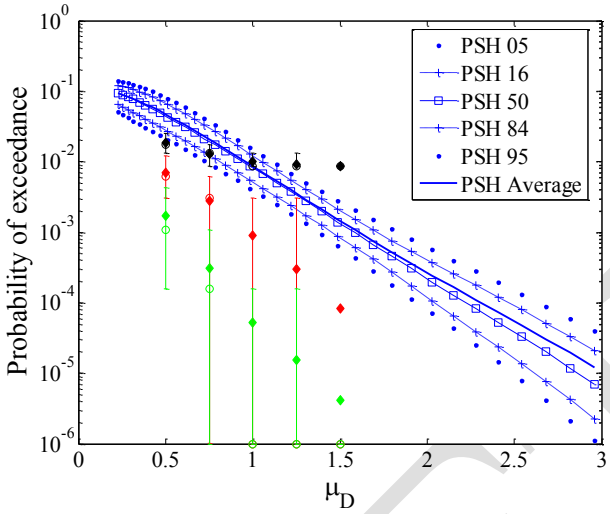


**Figure 4.6. Comparison of PSH predictions of different percentiles with meaningful statistics of the best-estimate (red) and of the upper (black) and lower (green) 90% confidence limits of the empirically-derived annual rates of exceedance of predefined mean damage levels (Marseille). Diamonds: average; circles: median; error bars: 5$^{th}$ and 95$^{th}$ percentiles.**

## 4.3 Comparison for aggregated sites

Applications of site-specific comparisons pointed out some critical aspects to be carefully accounted for. Results are affected by the seismic history of the selected sites, mostly characterised by a limited number of observations and/or by low intensity levels, as emerged from the analysis of the macroseismic data available in the study territory. Furthermore, a possible limitation may be represented by the potentially short observation time window. Both these issues can be addressed by sampling in space. Under the assumption that the process of occurrence of earthquakes is ergodic (a commonly accepted approximation), time and space can be swapped. An ergodic random process is one for which the time average of one sequence of events is the same as the ensemble average. In other terms, as it is not possible to have a sufficient number of observations corresponding to different earthquakes hitting a given site, different sites are aggregated and treated as if they were a single site. Based on these considerations, a methodology for comparing PSH results with observations by aggregating multiple sites was presented in Rosti *et al.* [2014]. Similarly to Tasan *et al.* [2014], the proposed procedure was aimed at comparing the observed and expected number of sites with exceedance of preselected PGA thresholds. Coherently with the comparison at individual sites, such methodology could be firstly improved by comparing the observed and expected number of sites with exceedance of preselected mean damage thresholds. Essentially, for each site to be aggregated, instead of generating an equivalent PGA history, an equivalent mean damage history could be derived, according to the procedure outlined in Chapter 2. Starting from the equivalent mean damage catalogues, the same steps presented in Rosti *et al.* [2014] can be then applied.

However, the results of this type of comparison are not further discussed here, for the reasons reported in the following. It is reckoned that, when sampling in space, the stochastic dependence

of observations generated at different sites by the same seismic event represents a critical aspect. To this aim, in Rosti *et al.* [2014], sites sufficiently far from each other were selected and dependent observations were systematically checked and eventually removed. Nevertheless, the assumption of stochastic independence of observations is a quite strong hypothesis, whereas the treatment of stochastic dependency is not an easy task. Iervolino and Giorgio [2015] showed that overlooking the stochastic dependency affecting observations generated by the same seismic event at different sites may lead to erroneous conclusions on the adequacy of the PSH model to be tested. However, they also showed that, bearing in mind that sites are not independent, treating them like that, i.e. overlooking the stochastic dependence, does not affect the mean but only the variance of a distribution of results [Iervolino and Giorgio, 2015]. Based on these considerations, a procedure for sampling in space, which does not require the assumption of stochastic independence of the sites, is proposed in the following. This methodology is indeed based on the comparison of mean annual rates of exceedance of preselected mean damage thresholds in at least one of the selected sites. In particular, the empirically-derived mean rates are compared with the predicted ones. As an example of application, the methodology is applied to the seven sites that were considered in Rosti *et al.* [2014], namely Annecy, Albertville, Draguignan, Beaumont de Pertuis, Digne, La Mure and L'Argentières La Bessée. For each site, Figure 4.7 shows the seismic history accounting for uncertainty in the intensity levels.

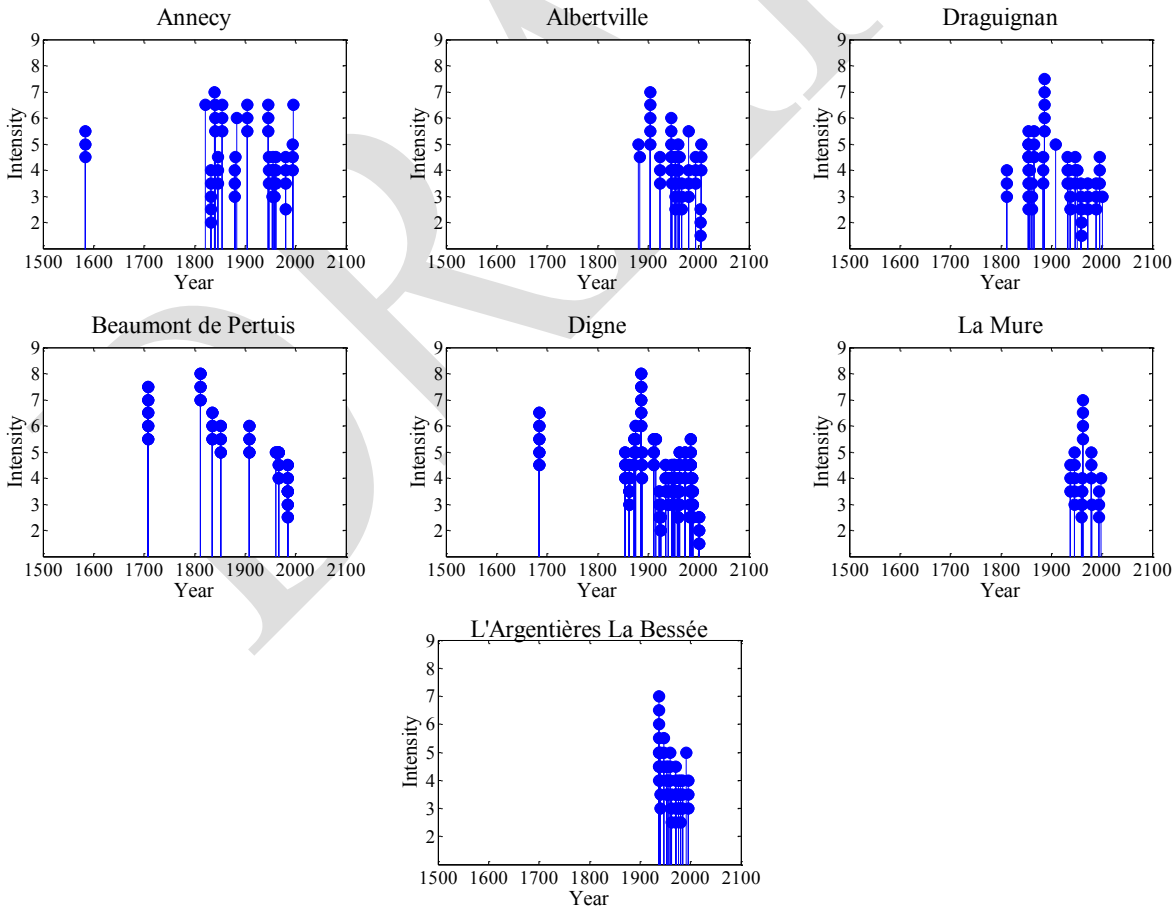


**Figure 4.7. Seismic histories accounting for uncertainty in the intensity levels, for each selected site.**

Based on the environmental category of each site, Table 4.1 summarises the weights attributed to each selected building typology, accounting for the subdivision of the building stock in the different structural typologies (Table 2.1). For each site, an equivalent mean damage history (Figure 4.8) is then derived through the procedure presented in Chapter 2.

**Table 4.1. Environmental categories associated with each site and weights accounting for the subdivision of the building stock in the selected building typologies.**

| Site | Category | $w_{typ1}$ | $w_{typ2}$ | $w_{typ3}$ | $w_{typ4}$ |
|---|---|---|---|---|---|
| Annecy | City | 0.05 | 0.50 | 0.15 | 0.30 |
| Albertville | Village in the Alps | 0.10 | 0.60 | 0.10 | 0.20 |
| Draguignan | City | 0.05 | 0.50 | 0.15 | 0.30 |
| Beaumont de Pertuis | Smaller village | 0.10 | 0.70 | 0.15 | 0.05 |
| Digne | Smaller village | 0.10 | 0.70 | 0.15 | 0.05 |
| La Mure | Village in the Alps | 0.10 | 0.60 | 0.10 | 0.20 |
| L'Argentières La Bessée | Smaller village | 0.10 | 0.70 | 0.15 | 0.05 |

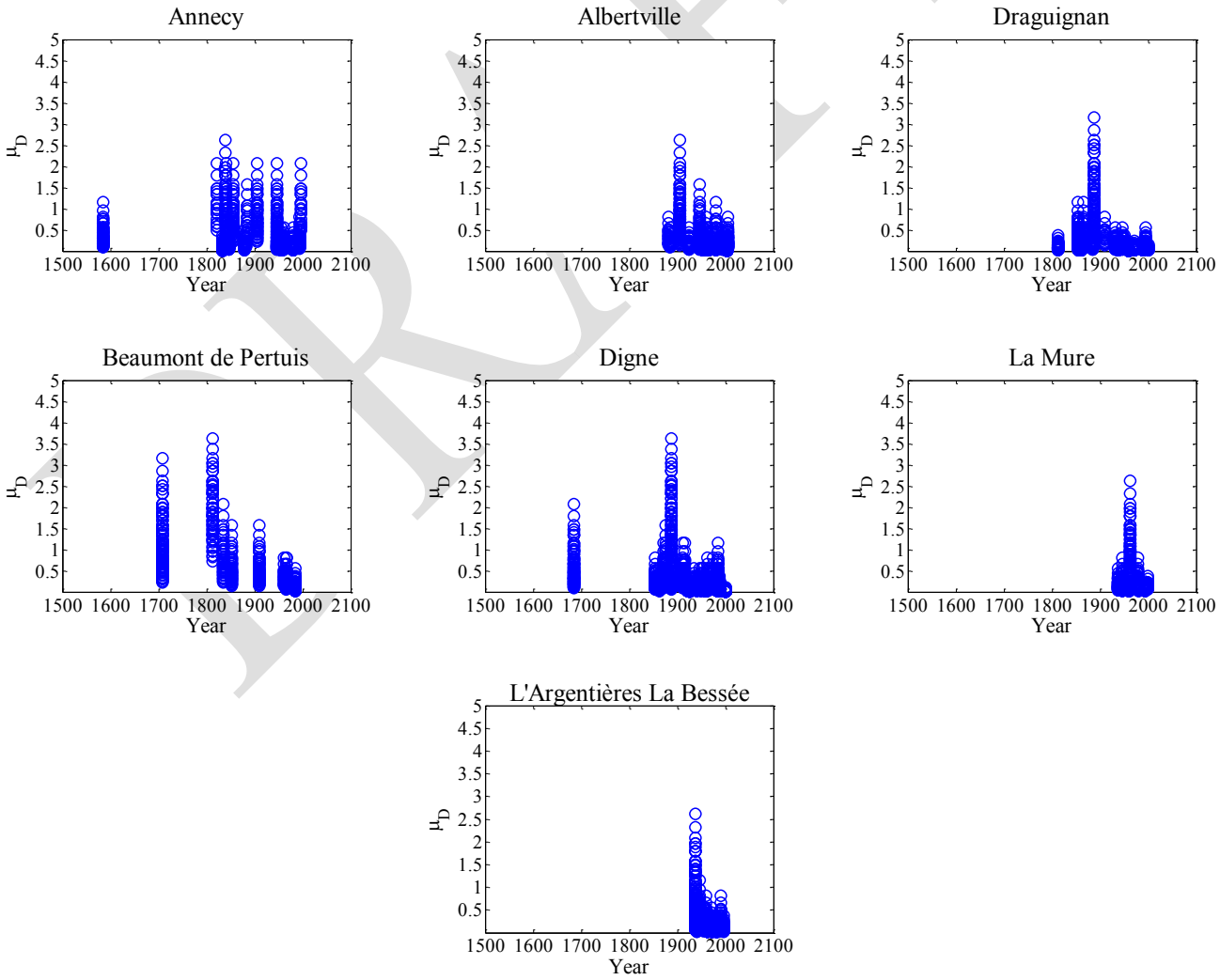


**Figure 4.8. Equivalent mean damage history of each selected site.**

Mean damage values are then sampled from the equivalent mean damage history of each site by means of a Monte Carlo approach. For a given site, the annual rates of exceedance of preselected mean damage thresholds are computed at each run, according to the procedure described in Section 2.7. To this aim, ten mean damage thresholds, ranging from 0.25 to 2.75 with an increment of 0.25, were considered. The Monte Carlo method is repeated many times so that, for a given site and for each mean damage level, a distribution of empirically-derived rates of exceedance is obtained. Then, for each site, the mean annual rate of exceedance of each mean damage threshold can be easily computed. The annual rate of exceedance of the preselected mean damage thresholds is then computed by summing the mean annual rates of exceedance of mean damage thresholds of the different sites. The result of the sum is then divided by the number of sites to be aggregated, in order to obtain the empirically-derived annual rate of exceedance of mean damage thresholds in at least one of the selected sites.

On the other side, specific treatment is required by PSH estimates, in order to allow a consistent comparison with empirical results. The epistemic uncertainty in the hazard estimates is accounted for by fitting lognormal distributions through the different percentiles of the available PSH predictions for each preselected mean damage threshold [Rota *et al.*, 2014]. For each site and for each mean damage threshold, annual rates of exceedance are then sampled from the corresponding approximating lognormal distribution. As shown in Figure 4.9, the lognormal distribution seems to provide a close approximation to the PSH predictions. The figure compares indeed discrete values of PSH rates of exceedances (diamonds) with those obtained through the lognormal approximation (squares), for the two example sites of Annecy and Draguignan.

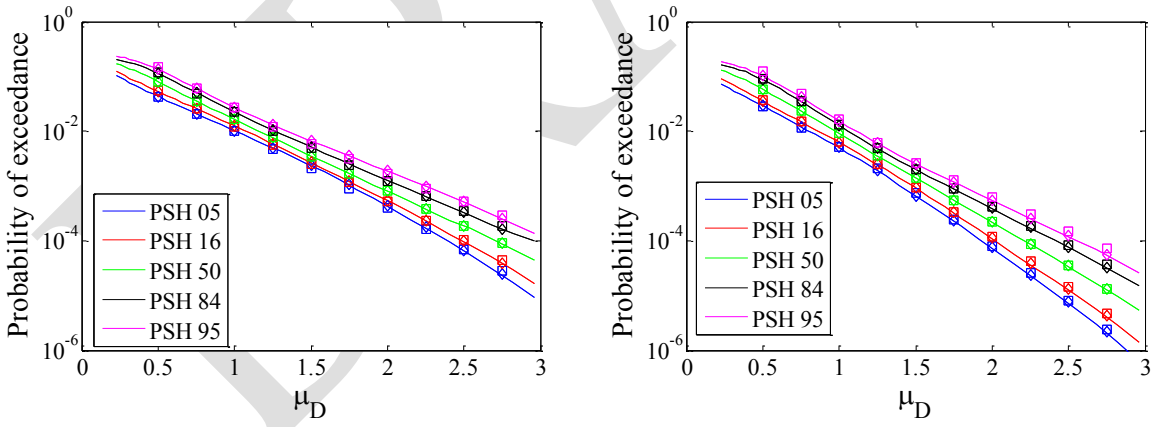


**Figure 4.9. Comparison of discrete PSH rates of exceedances (diamonds) with those obtained from the lognormal approximation (squares) for Annecy (left) and Draguignan (right).**

For each site and for each mean damage level, the sampled annual rates of exceedance are then averaged to derive mean annual rates of exceedance. The expected annual rate of exceedance of mean damage thresholds in at least one of the selected sites is then computed by summing the mean rates of exceedance of each site and dividing the result by the number of selected sites.

Figure 4.10 compares the empirically-derived annual rates of exceedance of preselected mean damage thresholds in at least one of the selected sites (red stars) against the expected ones (black). It is observed that, starting from a mean damage threshold equal to 1.5, PSH estimates are consistent with historical observations, as the ratio of the PSH-derived over the empirically-derived annual rates of exceedance in at least one of the selected sites is approximately 1. Conversely, PSH predictions overestimate empirical results at the lower mean damage thresholds. Results obtained from this application are in agreement with those presented in Rosti *et al.* [2014], although a different metric was considered in the comparison. In both cases, the discrepancy of PSH model with observations observed at lower ground motion intensity levels could be explained by the fact that some low intensity observations may not be reported in the historical catalogue.

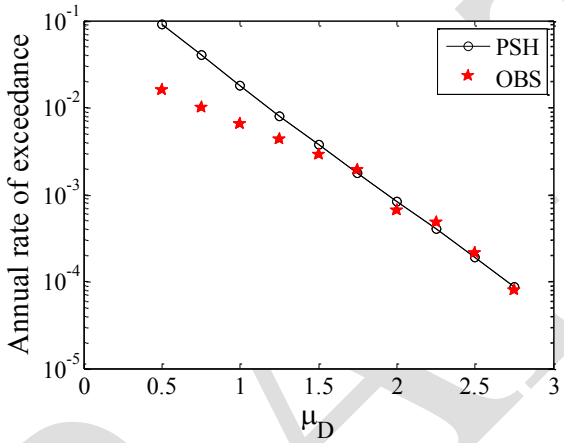


**Figure 4.10. Comparison of the empirically-derived and PSH-derived annual rates of exceedance of mean damage levels in at least one of the seven selected sites.**

## 4.4 Comparison at the regional scale level

As highlighted in Section 4.3, sampling in space can represent a possible solution for counteracting the limited availability of macroseismic data at individual sites. This represents a critical issue for most of the sites located in the South-East French territory, for which analyses of the French historical catalogue pointed out the lack of macroseismic observations of engineering interest. Collecting and gathering together information available at different sites have the clear potentiality of significantly enlarging the size of the available dataset.

Based on these preliminary considerations, a methodology for comparing PSH results with observations at the regional scale level was developed, starting from the approach proposed by Labbé [2010]. The originality of the proposed procedure lies in the generation of a set of spatially correlated random fields of PGA, constrained to the available macroseismic intensity observations, according to the procedure outlined in Rosti *et al.* [2014]. These random fields allow the derivation of distributions of PGA, compatible with the historical observations, representing the ground motion that should have been experienced at the considered sites, due to the occurrence of selected seismic events. For the implementation of the methodology two main ingredients are hence required, namely the selection of the sites to be considered in the application at the regional scale and the selection of the seismic events to be used in the random

field approach. Criteria for selection of both such ingredients are discussed in Sections 4.4.1 and 4.4.2, respectively. The comparison is then intended to be performed in terms of the mean annual rate of exceedance of preselected PGA thresholds in at least one of the selected sites. To this purpose, specific treatment is required by both observations and PSH predictions, as discussed in Section 4.3. Results of the comparison at the regional scale level are finally reported and commented in Section 4.4.3.

### *4.4.1 Identification of the sites to be aggregated*

The selected study area includes the eleven South-East French departments (i.e. Alpes Maritimes, Hautes-Alpes, Haute-Savoie, Vaucluse, Savoie, Isère, Rhône, Drôme, Alpes de-Haute-Provence, Bouches du Rhône, Var) for which analyses of the seismic events and of the corresponding macroseismic observations were carried out [Rosti *et al.*, 2014]. This area includes 580 of the 858 grid points, approximately distributed at 10 km intervals, for which Carbon *et al.* [2012] provided PSH estimates. The other 165 points were excluded as they were falling in the Mediterranean Sea or in neighbouring countries. In addition, 113 points were discarded because they were located in adjacent French departments. To this purpose, shapefiles provided by the Institute National de L'information Géographique et Forestière (IGN) (http://professionnels.ign.fr/) were used. Figure 4.11 shows the grid points selected for the comparison at the regional scale level.

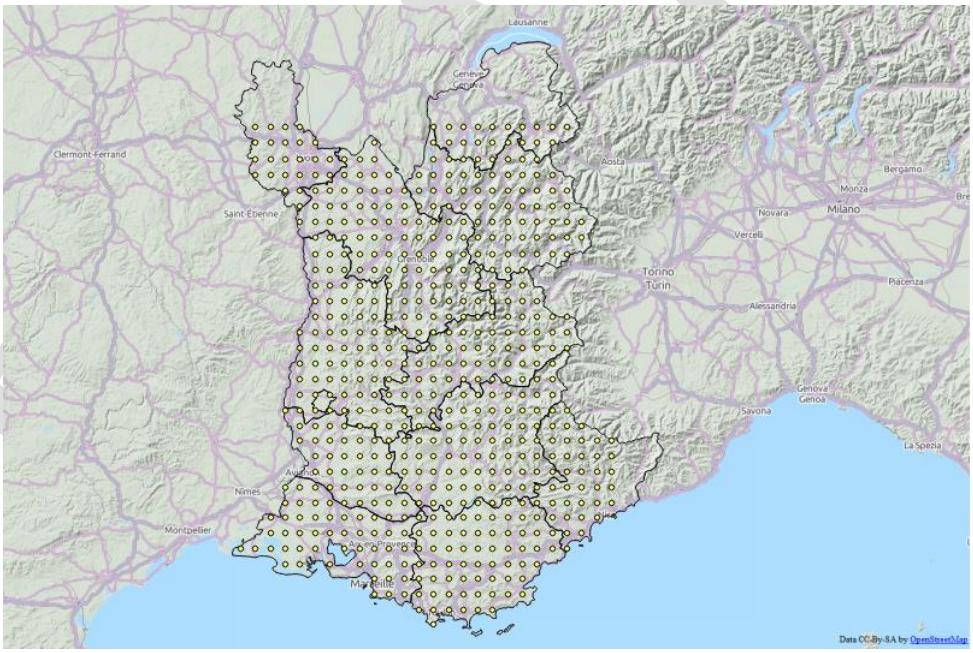


**Figure 4.11. Selected sites for the comparison at the regional scale level.**

### *4.4.2 Identification of the seismic events and generation of PGA random fields*

As previously anticipated, the originality of the developed procedure consists in generating a set of spatially correlated random fields of PGA, constrained to the available macroseismic intensity observations. The random fields approach essentially consists in modelling past earthquake scenarios consistently with the available seismological data and macroseismic

observations. To this purpose, it is necessary to identify a set of earthquakes for which synthetic observations are produced at the selected locations.

The criteria used for the selection of the seismic events considered for the application of the procedure are discussed in the following. First, all the seismic events (i.e. mainshocks, individual tremors and groups of tremors in a swarm) producing macroseismic intensity observations at least equal to 4 within the study area were identified. For each event, epicentral location and intensity were retrived from the Sisfrance online database. For the same events, moment magnitude values were collected from the SHEEC catalogue [Stucchi *et al.*, 2013], as they are not reported in the Sisfrance online database. For one of the earthquakes (i.e. the February 23rd 1941 Prazzo, Piemont, Italy earthquake) the moment magnitude value was instead retrieved from the Italian parametric catalogue [Rovida *et al.*, 2011]. For all the other seismic events not reported in the SHEEC catalogue, local magnitude values were computed by EDF-DIN-CEIDRE TEGG-Service Geologie Geotecnique. Events for which the epicentral intensity was not reported and/or without moment and local magnitude values were discarded.

For what concerns the earthquakes classified as individual tremor and groups of tremors in a swarm, for each swarm, only the events classified as mainshock in the SHEEC catalogue were taken into account. All the other dependent shocks were discarded. For the earthquakes not reported in SHEEC catalogue, the following criteria were adopted. If only one seismic event occurred in a given year, this event was considered. If instead more events of a same swarm occurred in a given year, only the earthquake with the highest epicentral intensity and magnitude values was accounted for.

Random fields were generated using the Akkar *et al.* [2014] ground motion prediction equation, together with the spatial correlation model of Jayaram and Baker [2009] (long range version). The Akkar *et al.* [2014] GMPE is considered applicable to the magnitude range from 4 to 8, for distances up to 200 km. Based on these considerations, only the seismic events with magnitude (moment magnitude if available, otherwise local magnitude) at least equal to 4 and located within 200 km of the hazard grid were considered. Furthermore, only seismic events with epicentral intensity at least equal to 5 were accounted for, in order to model only earthquakes that produced some level of damage on buildings. Finally, one of the resulting 197 events was discarded, as it occurred in 463 a.C. This choice was based on considerations on the completeness in time of the catalogue of seismic events which, apart from this very old event, only includes earthquakes in the period 1397-2005. The final dataset used to generate random fields of PGA hence included 196 seismic events of magnitude ranging from 4 to 6.62. Since the Akkar *et al.* [2014] GMPE was developed for moment magnitude, in the case of earthquakes for which the moment magnitude was not available, the equivalence of local and moment magnitudes was assumed, for the purpose of GMPE application. This is a fair assumption since the magnitude range of these seismic events is between 4 and 5.1 and, in this range, the two scales can be considered equivalent [Kramer, 1996].

A list of the seismic events selected for generating PGA random fields is reported in Annex 1. For each earthquake, date and time of occurrence, epicentral location and intensity and magnitude are specified. Earthquakes with epicentre outside France are in red.

Figure 4.12 (left) shows the time history of the selected events, with the corresponding magnitude value (i.e moment magnitude if available, local magnitude if the latter was not reported). Figure 4.12 (right) shows the epicentral intensity of each seismic event versus time. The color and size of the markers depend on the magnitude of the same event (i.e. green: 4≤M<5; orange: 5≤M<6; red: M≥6. Figure 4.13 shows the epicentral location of each earthquake. Still, the different color and size of the markers correspond to different ranges of magnitude, as in Figure 4.12.

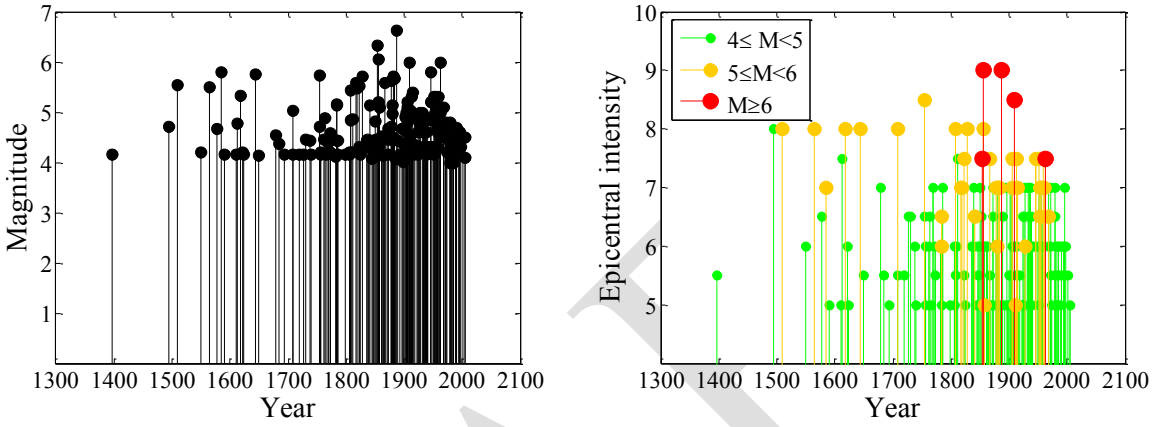


**Figure 4.12. Magnitude of the selected seismic events versus time (left) and epicentral intensity of the selected seismic events versus time(right).**

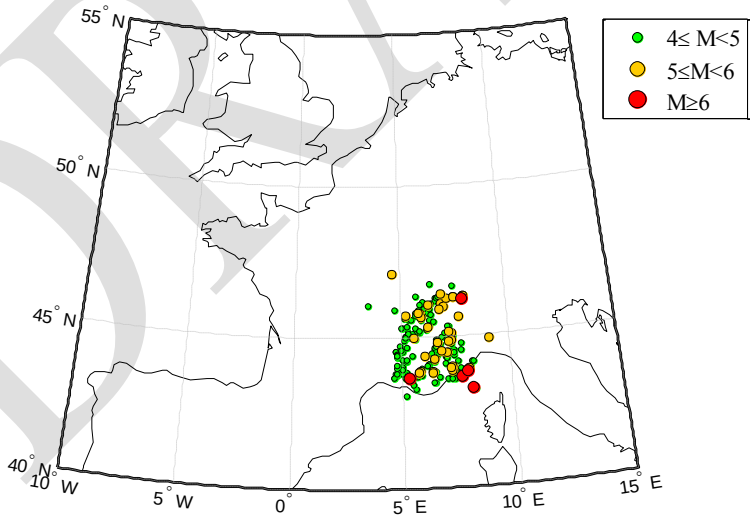


**Figure 4.13. Epicentre location of the selected seismic events, classified based on the magnitude range. Green: 4≤M<5; orange: 5≤M<6; red: M≥6.**

No finite fault models or fault type mechanism were available for the calculations. It was therefore decided to adopt the Akkar *et al.* [2014] model, developed for epicentral source-to-site distances and a default fault mechanism (strike-slip) in the calculations. The use of the

epicentral distance model was considered acceptable for most of the modelled events, which are either small earthquakes, for which the difference between distance from the epicentre and distance from the fault can be considered negligible, or larger events (five earthquakes with $M_w \geq 6$) which however occurred far away from the sites of interest. However, there are at least two cases (i.e. the June 11th 1909 Lambesc earthquake and the December 29th 1854 Riviera di Ponente, San Remo, Italy earthquake) with $M_w \geq 6$ and epicentre located within or near the calculation grid (less than 40 km), for which a finite fault model would be needed to improve the modelled ground motion field.

For all the selected earthquakes, the intensity points located at a distance smaller than 100 km from the grid points, with intensity at least equal to 4, were used as a constraint in the modelling of the random fields. The consideration of any intensity point located farther than 100 km from the sites for which the simulation is carried out would have no effect on the results of the simulation since, for the model used, the effects of spatial correlation of PGA from site to site decrease quickly with increasing inter-site distance, becoming almost irrelevant already beyond 30 km.

The random fields were developed for PGA on rock sites, consistently with the hazard study to be tested. The modelling was carried out in terms of normalised residuals of PGA calculated with respect to the selected GMPE model, in accordance with the procedure discussed in Rosti *et al*. [2014]. To calculate the normalised residuals of PGA for the PGA derived from the macroseismic intensity values, the knowledge of the soil type or shear wave velocity at the intensity locations is necessary. For this purpose, site conditions were evaluated based on the $V_{s,30}$ map produced by USGS [Wald and Allen, 2007], available at the website (http://earthquake.usgs.gov/hazards/apps/vs30/predefined.php#Europe).

For each considered seismic event, the simulated PGA random fields allow to obtain a probability distribution of PGA at the considered sites, which is compatible with the characteristics of the event and is conditioned on the available macroseismic observations. In particular, a lognormal distribution of PGA values was obtained at each site, for each seismic event considered.

### *4.4.3 Results of the comparison at the regional scale level*

The comparison at the regional scale level is simply carried out by comparing the empirically-derived and expected annual rates of exceedance of preselcted PGA thresholds, in at least one of the selected sites. Empirically-derived and expected annual rates of exceedance in at least one of the selected sites were computed based on the same procedure already discussed for the case of aggregated sites (Section 4.3). Also in this case, the issue of stochastic dependency of observations is overlooked and therefore the comparison is performed in terms of mean annual rates, in order to avoid the effect of the possible existing dependency on the results.

With respect to Section 4.3, there are some differences in the procedure for the calculation of the empirically-derived rates of exceedance of selected PGA thresholds in at least one of the selected sites. First, for each site, an equivalent seismic history in terms of synthetic PGA values was obtained, based on the results of the random fields approach. In particular, a lognormal distribution of PGA values was obtained for each event hitting the site and a single PGA value

was sampled from this distribution. For each site, the observation period was hence calculated for each site, as the difference between the year 2007 (i.e. the last year for which the French historical catalogue provides information) and the year of the first event hitting the site of interest. Finally, for each site, the mean annual rate of exceedance was computed for twenty PGA levels for which PSH estimates are available [Carbon *et al*., 2012] and ranging from 0.001 g to 1.02 g.

Figure 4.14 (left) compares the empirically-derived annual rates of exceedance of PGA thresholds in at least one of the selected sites with the expected ones. In the figure, red stars correspond to observations, whilst black circles correspond to PSH estimates. Also thanks to the logarithmic scale adopted in the plot, the comparison seems to provide very close results in the entire range of PGA. To better explore the consistency of the obtained rates of exceedance, the ratio of the PSH over the empirically-derived rates of exceedance was calculated, as shown in Figure 4.14 (right). In almost all cases the ratio is higher than 1, suggesting the tendency of PSH estimates of overestimating empirical results. In the 0.1 – 0.5g PGA range the ratio is approximately equal to 1, indicating a good agreement between PSH predictions and observations. The overestimation at lower PGA thresholds may be explained by the exclusion of seismic events with lower epicentral intensity and magnitude values from the list of events considered for the generation of random fields, although it is believed that these events would not significantly affect the results. Nevertheless, it can be noted that, selecting a value of the probability of exceedance (i.e. following the typical approach used for design), the overestimation in the corresponding acceleration is not so significant.

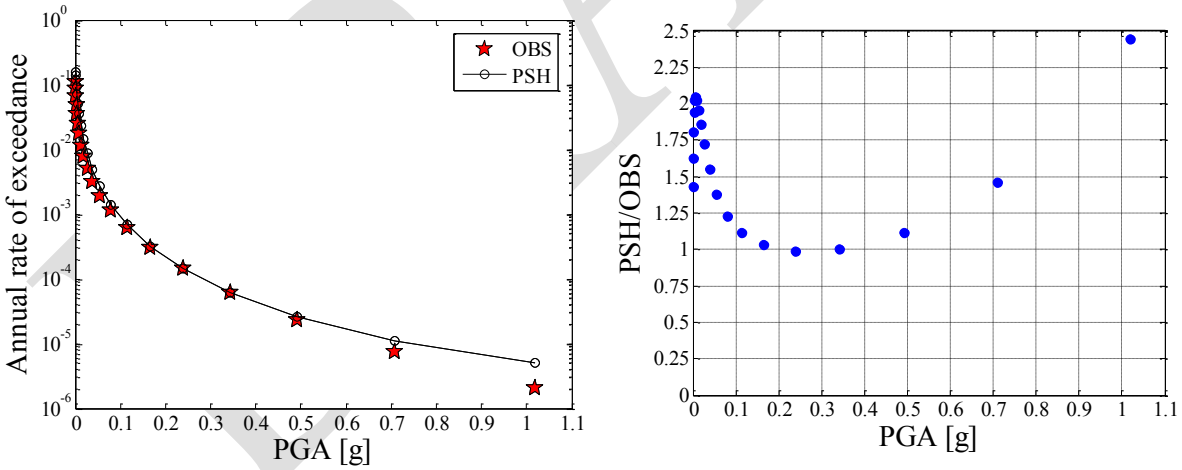


**Figure 4.14. Comparison of the empirically-derived and PSH-derived annual rates of exceedance in at least one of the selected sites (left) and ratio of PSH-derived over empirically-derived annual rates of exceedance in at least one of the selected sites (right).**

As already discussed, a comparison at the regional scale has the clear advantage of increasing the size of the available dataset, since all the information available within a study territory are considered. Nevertheless, such a comparison can only represent a test of the average consistency of PSH predictions with observations, not providing direct information on site-specific hazard.

# 5 CONCLUSIONS AND FURTHER DEVELOPMENTS OF THE WORK

Although the probabilistic methods used for seismic hazard prediction have been continuously developed and improved over the last decades, for regions with low-to-moderate seismicity like France, the reliability of these methods can still be improved through a better quantification of the uncertainties. The quality of the results can then be estimated by comparing predictions with observations.

This Chapter tries to summarise the steps carried out within this project towards a comparison of PSH results and historical macroseismic observations for South-East France, highlighting in particular the different issues encountered during the work and the possible further developments of this study.

The Chapter will recall the main aspects of the methodologies initially drafted in Rosti *et al.*, [2014] and then further developed as discussed in this report, focusing on the strengths and weaknesses of each step. Suggestions are also provided for future developments aiming at possibly overcoming some of the limitations of the approach adopted in this work.

Since the PSH results developed within the SIGMA Project [Carbon *et al.*, 2012] were provided for PGA thresholds, the first straightforward choice would have been to compare PSH predictions with observations by using accelerometric data. Despite the limited uncertainty associated with recorded accelerations, the short lifetime of accelerometric stations, with respect to the observation period that would be necessary for events with large return periods, represents a severe limitation of the available data. As a possible alternative, macroseismic observations could be seen as records of "imperfect instruments" recording ground motion. They inevitably bear significant uncertainty and subjectivity, but they are available for longer observation periods, especially in case of countries with a long civilization history, like France. Moreover, in this particular case, macroseismic intensities were not directly used as input data for the PSH models developed for France. For this reason, they can be seen as an independent set of data, which could be used to test the results of PSHA studies. Based on these considerations, it was decided to compare PSH results with historical macroseismic observations.

The first step of the work hence consisted in collecting and analysing all available information on the historical seismicity of the study area, including eleven South-East French departments.

This information was reported in the French historical seismic catalogue Sisfrance. Analysis of the data pointed out the need for a better characterisation of the historical seismicity of the selected territory. Focusing on the seismic events, a better characterisation is required, at least for the major earthquakes. Magnitude values should be reported in the online database and clarifications should be provided for the seismic events labelled as "swarms". For instance, it could be useful to provide specific tags for distinguishing the main from the dependent shocks, similarly to the SHEEC catalogue [Stucchi *et al.*, 2013]. Also, severe limitations affecting the completeness in time of the French catalogue were highlighted by looking at the evolution in time of the rates of occurrence of earthquakes of different intensity. If possible, the completeness in time of the database should be extended by studying historic documentary sources, at least for a restricted area of interest.

Moreover, a limited amount of damaging earthquakes was observed, implying low percentages of macroseismic observations with intensity level at least equal to 6 (i.e. the intensity degree corresponding to slight damage on structures, according to the MSK scale). Furthermore, higher macroseismic intensity levels were typically associated with foreign earthquakes and inconsistencies in the intensity evaluations provided by Sisfrance and by neighbouring countries were observed [Rovida, 2013; Scotti, 2013]. In particular, the intensity levels reported in Sisfrance seem to be generally higher than the corresponding values provided by other foreign databases (e.g. the Italian macroseismic database DBMI11, Locati *et al.*, 2011). These inconsistencies suggested further investigations, at least oriented to the homogenisation of macroseismic data due to earthquakes at the borders. Applications of intensity prediction equations for some events suggested possible missing macroseismic observations in the seismic histories of several sites and possible overestimation/underestimation of some intensity evaluations. In this sense, the generation of synthetic observations based on conditional simulation of random fields of ground motion may represent an effective tool for integrating the historical catalogue.

A methodology for converting macroseismic intensities into PGAs, accounting for several sources of uncertainty, was first developed, as discussed in Rosti *et al.* [2014]. The implementation of the procedure required two fundamental ingredients, namely the collection of macroseismic intensities observed at a given site and information on the subdivision of the historical building stock into different structural typologies. To this purpose, a number of sites, for which more detailed information on macroseismic observations and old building stock were available, were selected. The conversion of macroseismic intensities into PGAs was performed by using empirical fragility curves, derived from statistical analysis of post-earthquake damage data collected after several Italian earthquakes [Rota *et al.*, 2008]. Some issues related to the selected curves were identified. Firstly, the fragility curve corresponding to damage level DS5 was missing for some building typologies, due to the limited amount of empirical data corresponding to those particular cases. Furthermore, due to the lack of empirical data at higher PGA levels, the range of validity of the adopted fragility curves was restricted to 0.3 g. Both these weaknesses were solved by developing a new set of fragility curves, using an extended database in which the post-earthquake damage data collected after L'Aquila event (2009) were added. This consisted of a significant number of empirical data corresponding to higher PGAs and allowed extending the limit of validity of the available curves up to 0.5 g. Despite this

significant improvement, the fragility curves finally adopted still present some limitations, mainly related to the presence of endemic (pre-existing) damage biasing the available set of data and affecting the reliability of these curves, particularly in the low-PGA range of interest for South-East France.

A critical aspect of the methodology presented in Rosti *et al.* [2014] for converting macroseismic observations into PGAs concerned the application of fragility curves in the opposite sense, i.e. by converting the independent into the dependent variable, without properly considering the residuals of the regression. This issue was solved in the updated methodology presented in this report, which is based on a different metric of the comparison. Indeed, the comparison is no longer carried out in terms of the rate of exceedance of selected PGA thresholds, but rather on the rate of exceedance of mean damage levels (i.e. the average damage expected in the old building stock). This approach is still based on the use of fragility curves, but it does not require the inversion of these curves, hence allowing to correctly take into account the residuals of the regressions.

In both versions, the methodology for converting macroseismic intensities into a quantity to be directly compared with PSHA results allowed to take into account several sources of uncertainty, related with the reliability of macroseismic intensity values, the subdivision of the building stock into different structural typologies and the attribution of the building typologies to the EMS-98 vulnerability classes. On one side, the proposed procedure has the advantage to account for all the possible epistemic uncertainties. On the other, it is reckoned that the combination of several sources of uncertainty may result in highly scattered results. This aspect was investigated in depth in Rosti *et al.* [2014], by comparing for example the scatter in the values of PGA obtained from the conversion of macroseismic intensities with the one provided by intensity to PGA conversion relationships available in the literature. The two dispersions turned out to be of the same order of magnitude. Also, the analyses discussed in Rosti *et al.* [2014], showed that most of the uncertainty observed in the results of the comparison was due to the shape of the first adopted version of the fragility curves, consequently affecting the shape of the mean damage curve. Some sensitivity studies were then carried out to assess the influence of each source of uncertainty on the final results. Based on these results, some choices were possible regarding the different options of the proposed methodology, allowing to narrow the uncertainty bound on the results of the comparison. Moreover, the adoption of mean damage as the metric of the comparison, avoiding the issue of inversion of the fragility curves, allowed a significant reduction of the dispersion in the obtained results, expressed in terms of rates of exceedance of mean damage levels.

Comparison of PSH results with observations was first carried out at individual sites. Site-specific comparison is straightforward as it consists in directly comparing the empirically-derived rates of exceedance of selected thresholds of the metric of the comparison (in this case, the mean damage), with the PSH predictions of a given site. This may represent a natural choice for sites of particular interest, for example due to the presence of nuclear installations, for which a direct and immediate comparison of PSH predictions with observations could be worthwhile. Nevertheless, site-specific comparisons are unavoidably affected by the seismic history of the selected site. In the study area, the very limited number of macroseismic data of engineering

interest emerged from the analysis of the SisFrance database turned out in many cases to strongly affect the comparison at single sites, often preventing pertinent comparisons with PSH results. Furthermore, the potentially short observation period at single sites, possibly also affected by the incompleteness of the catalogue, represents an additional limitation of the comparison for single sites, as it limits the return period for which the results of the comparison can be considered reliable.

These considerations suggested to carry out the comparison at a larger scale, by aggregating several sites, based on the concept of sampling in space. This is based on the assumption of ergodicity of the process of earthquakes' occurrence, a commonly accepted approximation which allows to swap time and space. Given that the different sites can be assumed to be affected by observations due to independent earthquakes, the assumption of ergodicity allows to enlarge the observation time window. In this approach, sites with longer observation periods have more influence on the total observation period, given by the sum of the observation time windows of each selected site. As a consequence, their seismicity has a stronger effect on the results of the comparison. With this hypothesis, a methodology for aggregating multiple sites was developed by Rosti *et al.* [2014], following an approach similar to the one proposed by Tasan *et al.* [2014], consisting in comparing the observed and the expected number of sites with exceedance of preselected PGA thresholds. The methodology was tentatively applied to seven sites of the South-East French territory, sufficiently far from each other so that exceedances at the different sites could be assumed to be stochastically independent. Also, dependent observations were systematically checked and eventually removed.

However, this methodology requires as a fundamental requisite that the sites are affected by independent events. According to Iervolino and Giorgio [2015], neglecting the effect of stochastic dependence of observations generated at different sites by the same earthquake may lead to fallacious conclusions on the adequacy of PSH models. However, they showed that, bearing in mind that sites are not independent, treating them like that, i.e. overlooking the stochastic dependence, does not affect the mean but only the variance of a distribution of results [Iervolino and Giorgio, 2015].

For this reason, in this report the comparison on aggregated sites as well as the comparison at the regional level, were carried out only with reference to the mean annual rate of exceedance of selected ground motion levels in at least one of the considered sites. This allows to avoid the assumption on the stochastic independence of the sites, which was instead at the basis of the methodology for the comparison on aggregated sites initially proposed in Rosti *et al.* [2014], based on the comparison of the number of sites with exceedance.

The trial application of the methodology showed the tendency of PSH results of overestimating the number of sites with exceedance at the lower levels of ground motion. This could be explained by the fact that some low intensity macroseismic observations may be missing from the catalogue. To this aim, the quality of estimation of lower ground motion thresholds could be improved by integrating recorded accelerations in the procedure.

The aggregation of multiple sites pointed out the opportunity of making up for the limited availability of macroseismic data at individual sites. Sampling in space also suggested the

development of a method for the comparison at the regional scale level, similarly to the approach proposed by Labbé [2010]. Comparing PSH results with observations at the regional scale level allows to significantly increase the size of the available macroseismic dataset, as all the historical observations in the study region are pooled together. On the other side, such a comparison can only represent a test of the average consistency of the PSH results with observations, not providing direct information for individual sites. Its application hence requires the identification of areas of rather homogeneous seismicity. Also in the comparison at the regional scale, where thousands of sites are aggregated, sites are obviously not stochastically independent. They can be handled as independent, provided that the method works in terms of mean annual rates, allowing to avoid drawing erroneous conclusions on the adequacy of a given PSH model.

An example of preliminary application of the proposed approach at the regional level was presented in this report and allowed to identify several aspects that could be improved in future developments of the work. This tentative application took advantage of the theory of random fields of ground motion, described in Rosti *et al.* [2014], to integrate the available database of observations by means of conditional simulations of the PGA levels expected at the nodes of the adopted grid of sites for the different historical earthquakes affecting the area.

As a first improvement of the methodology, the comparison could be applied to sub-regions of the area of interest characterized by a roughly homogeneous seismicity level, hence reducing the smoothing effect due to the adoption of an "average" comparison. Also, a possible improvement could consist in developing a complete distribution of the rates of exceedance of different PGA levels, taking properly into account the stochastic dependency of the different sites by means of simulations. Consideration of the spatial correlation of ground motion at the different sites could also improve the definition of seismic hazard. Finally, as already mentioned, the adopted empirical fragility curves present a number of issues, which could affect the results in particular for the low levels of ground motions typical of the French seismicity. The development of analytical fragility curves, derived by means of nonlinear analyses of building prototypes representative of the French historical building stock could possibly allow to solve some of these issues, with the additional possible advantage of reducing the obtained variability in the results.

# REFERENCES

Akkar, S., Sandikkaya, M. A., Bommer J. J. [2014] "Empirical ground-motion models for point- and extended- source crustal earthquake scenarios in Europe and the Middle East", *Bulletin of Earthquake Engineering*, Vol. 12, No1, pp 359-387.

Albarello, D., D'Amico, V. [2008] "Testing probabilistic seismic hazard estimates by comparison with observations: an example in Italy," *Geophysical Journal International*, Vol. 175, pp. 1088-1094.

Baker, J. W., Abrahamson, N. A., Whitney, J. W., Board, M. P., Hanks, T. C. [2013] "Use of Fragile Geologic Structures as Indicators of Unexceeded Ground Motions and Direct Constraints on Probabilistic Seismic Hazard Analysis," *Bulletin of the Seismological Society of America*, Vol. 103, No. 3, pp. 1898-1911.

Beauval, C. [2011] "On the use of observations for constraining probabilistic seismic hazard estimates – brief review of existing methods," *International Conference on Application of Statistics and Probability in Civil Engineering*, Zurich, Switzerland.

Braga, F., Dolce, M., Liberatore, D. [1982] "A statistical study on damaged buildings and an ensuing review of the MSK76 scale," *Proceedings of 7th European Conference on Earthquake Engineering*, Athens.

Brune, J. N. [1996] "Precariously Balanced Rocks and Ground-Motion Maps for Southern California," *Bulletin of the Seismological Society of America*, Vol. 86, No. 1A, pp. 43-54.

Carbon, D., Drouet, S., Gomes, C., Leon, A., Martin, C., Secanell, R. [2012] "Probabilistic analysis for France's southeast ¼ to produce a preliminary "classical" hazard map," Deliverable SIGMA-2012-D4-24, Final Report.

Dubois, D., Prade, H. [1980] *Fuzzy Sets and Systems*, Academic Press, New York.

Grünthal, G. (ed) [1998] "European Macroseismic Scale 1998 (EMS 1998)," *Council of Europe, Cahiers du Centre Européen de Géodynamique et de Sismologie*, Vol. 15.

Iervolino, I. [2013] "Probabilities and Fallacies: Why Hazard Maps Cannot Be Validated by Individual Earthquakes," *Earthquake Spectra*, Vol. 29, No. 3, pp. 1125-1136.

Iervolino, I., Giorgio, M. [2015] "The effect of dependence of observations on hazard validation studies," *Proc CSNI Workshop on "Testing PSHA Results and Benefit of Bayesian Techniques for Seismic Hazard Assessment*, 4-6 February, Pavia, Italy.

Jayaram, N., Baker, J. W. [2009] "Correlation model for spatially distributed ground-motion intensities," *Earthquake Engineering and Structural Dynamics*, Vol. 38, No 15, pp. 1687-1708.

Kramer, S. L. [1996] *Geotechnical Earthquake Engineering*, Prentice Hall, pp 653.

Labbé, P. B. [2010] "PSHA outputs versus historical seismicity Example of France," *Proceedings of 14th European Conference on Earthquake Engineering*, Ohrid, Macedonia.

Lagomarsino, S., Giovinazzi, S. [2006] "Macroseimic and mechanical models for the vulnerability and damage assessment of current buildings," *Bulletin of Earthquake Engineering*, Vol. 4, pp. 415-443.

Levenberg, K. [1944] "A method for the solution of certain non-linear problems in least squares," *Quarterly of Applied Mathematics*, Vol. 2, No. 2, pp. 164–168.

Locati, M., Camassi, R., Stucchi, M. (eds) [2011] "DBMI11, the 2011 version of the Italian Macroseismic Database," Milano, Bologna, http://emidius.mi.ingv.it/DBMI, DOI: 10.6092/INGV.IT-DBMI11.

Marquardt, D.W. [1963] "An algorithm for the least-squares estimation of nonlinear parameters," *SIAM Journal of Applied Mathematics*, Vol. 11, No. 2, pp. 431–441.

Medvedev, S., Sponheuer, W., Karník, V. [1964] "Neue seismische Skala Intensity scale of earthquakes,7. Tagung der Europäischen Seismologischen Kommission vom 24.9. bis 30.9.1962. In: Jena, Veröff. Institut für Bodendynamik und Erdbebenforschung in Jena," *Deutsche Akademie der Wissenschaften,* Vol. 77, pp 69-76.

Mucciarelli, M. [2014] Personal communication.

Musson, R. M. W., Grünthal G., Stucchi, M. [2010] "The comparison of macroseismic intensity scales," *Journal of Seismology*, Vol. 14, pp. 413-428.

OECD [2007] "Specialist meeting on SPSA for nuclear facilities," NEA/CSNI/R(2007)14, Paris.

Purvance, M. D., Brune, J. N., Abrahamson, N. A., Anderson, J. G. [2008] "Consistency of Precariously Balanced Rocks with Probabilistic Seismic Hazard Estimates in Southern California," *Bulletin of the Seismological Society of America*, Vol. 98, No. 6, pp. 2629-2640.

Rosti, A., Rota, M., Fiorini, E., Penna, A., Bazzurro, P., Magenes, G. [2014] "Deliverable on the research activity between EUCENTRE and Areva for the Sigma project WP4 Task 3: development and implementation of a method to compare psha results to historical observations using fragility curves" Revised version of the intermediate report.

Rota, M., Penna, A, Strobbia, C.L. [2008a] "Processing Italian damage data to derive typological fragility curves," *Soil Dynamics and Earthquake Engineering*, Vol. 28, No. 10-11, pp. 933-947.

Rota, M., Penna, A., Strobbia, C. and Magenes G. [2008b] "Derivation of empirical fragility curves from Italian damage data," Research Report No. ROSE-2008/08, IUSS Press, Pavia, ISBN: 978-88-6198-029-7, pp. 240.

Rota, M., Penna, A, Magenes, G. [2014] "A framework for the seismic assessment of existing masonry buildings accounting for different sources of uncertainty," *Earthquake Engineering and Structural Dynamics*, Vol. 43, No. 7, pp. 1045-1066.

Rovida, A. [2013] "The Italian Macroseismic Database (DBMI11) at the Italian-French Border," *Workshop Macroseismicity: sharing and use of historical data*, 3 April 2013, Paris.

Rovida, A., Camassi, R., Gasperini, P., Stucchi, M. (eds) [2011] "CPTI11, the 2011 version of the Parametric Catalogue of Italian Earthquakes," Milano, Bologna, http://emidius.mi.ingv.it/CPTI, DOI: 10.6092/INGV.IT-CPTI11.

Scotti, O. [2013] "Joining forces/efforts to improve our knowledge of the effects of earthquakes affecting France and neighbouring countries," *Workshop Macroseismicity: sharing and use of historical data*, 3 April 2013, Paris.

SisFrance - Catalogue des séismes français métropolitains, BRGM, EDF, IRSN, www.sisfrance.net.

Stein, S., Geller, R., Liu, M. [2011] "Bad Assumptions or Bad Luck: Why Earthquake Hazard Maps Need Objective Testing," *Seismological Research Letters*, Vol. 82, No. 5, pp. 623-626.

Stirling, M. W. [2012] "Earthquake Hazard Maps and Objective Testing: The Hazard Mapper's Point of View," *Seismological Research Letters*, Vol. 83, No. 2, pp. 231-232.

Stirling, M., Gerstenberger, M. [2010] "Ground Motion-Based Testing of Seismic Hazard Models in New Zealand," *Bulletin of the Seismological Society of America*, Vol. 100, No. 4, pp. 1407-1414.

Stirling, M., Petersen, M. [2006] "Comparison of the Historical Record of Earthquake Hazard with Seismic-Hazard Models for New Zealand and the Continental United States," *Bulletin of the Seismological Society of America*, Vol. 96, No. 6, pp. 1978-1994.

Stucchi, M. et al. [2013] "The SHARE European Earthquake Catalogue (SHEEC) 1000 - 1899," *Journal of Seismology*, Vol. 17, No 2, pp. 523–544.

Tasan, H., Beauval, C., Helmstetter, A., Sandikkaya, A., Guéguen, P. [2014] "Testing probabilistic seismic hazard estimates against accelerometric data in two countries: France and Turkey," *Geophysical Journal International*, Vol. 198, No. 3, pp. 1554-1571.

Wald, D. J., Allen, T. I. [2007] "Topographic slope as a proxy for seismic site conditions and amplification," *Bulletin of the Seismological Society of America*, Vol. 97, No. 5, pp. 1379-1395.

Ward, S. N. [1995] "Area-Based Tests of Long-Term Seismic Hazard Predictions," *Bulletin of the Seismological Society of America*, Vol. 85, No. 5, pp. 1285-1298.

# ANNEX 1: LIST OF SEISMIC EVENTS CONSIDERED FOR THE GENERATION OF RANDOM FIELDS

The table lists the seismic events considered for the generation of PGA random fields, whose results are used for the comparison at the regional scale discussed in Chapter 4. For a discussion of the criteria followed to select these seismic events, the reader is referred to section 4.4.

For each earthquake, date and time of occurrence, epicentral location and intensity and magnitude are specified. Earthquakes with epicentre outside France are indicated in red.

| Date | Time | Epicentre location | $I_{epc}$ | M |
|---|---|---|---|---|
| 31 October 2005 | 3 h 39 min 59 sec | VALLEE DE L'ARLY (N. ALBERTVILLE) | 5 | 4.10 |
| 8 September 2005 | 11 h 27 min 18 sec | MASSIF DU MONT-BLANC (VALLORCINE) | 5 | 4.50 |
| 25 February 2001 | 18 h 34 min 44 sec | MEDITERRANEE (S-E NICE) | 5.5 | 4.50 |
| 31 October 1997 | 4 h 23 min 44 sec | PREALPES DE DIGNE (PRADS-HAUTE-BLEONE) | 6 | 4.30 |
| 15 July 1996 | 0 h 13 min 31 sec | AVANT-PAYS SAVOYARD (EPAGNY-ANNECY) | 7 | 4.60 |
| 21 April 1995 | 8 h 2 min 56 sec | RIVIERA DI PONENTE (VINTIMILLE) | 6 | 4.40 |
| 14 December 1994 | 8 h 56 min | GENEVOIS (LES VILLARDS-SUR-THONES) | 6 | 4.30 |
| 11 February 1991 | 15 h 43 min 45 sec | BRIANCONNAIS (BRIANCON) | 6 | 4.20 |
| 11 February 1990 | 7 h 38 sec | PIEMONT (TORINO) | 5.5 | 4.70 |
| 26 December 1989 | 20 h | MEDITERRANEE (S. NICE) | 5 | 4.60 |
| 19 June 1984 | 11 h 40 min 37 sec | PREALPES DE DIGNE (AIGLUN) | 6 | 4.10 |
| 17 April 1984 | 8 h 53 min 39 sec | VERCORS (ROCHEFORT-SAMSON) | 5.5 | 4.00 |
| 19 February 1984 | 21 h 14 min 37 sec | BASSE-PROVENCE (MIMET) | 6 | 4.00 |
| 22 January 1983 | 12 h 51 min 57 sec | PIEMONT (SUSA) | 5 | 4.10 |
| 22 April 1981 | 4 h 26 min 22 sec | MEDITERRANEE (S. SAN REMO) | 6 | 4.50 |
| 8 February 1981 | 4 h 30 min 11 sec | PIEMONT (SUSA ?) | 5 | 4.40 |
| 2 December 1980 | 5 h 58 min 13 sec | BAUGES (FAVERGES) | 6.5 | 4.40 |
| 5 January 1980 | 14 h 32 min 28 sec | PIEMONT (PINEROLO) | 7 | 4.80 |
| 16 April 1979 | 12 h 27 min 12 sec | DIOIS (CHASTEL-ARNAUD) | 5.5 | 4.00 |
| 8 February 1974 | 20 h 12 min 17 sec | PREALPES DE DIGNE (THORAME) | 5 | 4.20 |
| 18 January 1972 | 23 h 26 min 19 sec | RIVIERA DI PONENTE (PIETRA LIGURE) | 6 | 4.80 |
| 21 June 1971 | 7 h 25 min 32 sec | JURA (VAUX-LES-SAINT-CLAUDE) | 7 | 4.50 |
| 1 February 1971 | 12 h 26 min 55 sec | PIEMONT (DRONERO) | 5.5 | 4.60 |
| 19 August 1968 | 0 h 36 min 43 sec | CHABLAIS (ABONDANCE) | 7 | 4.70 |
| 27 June 1968 | 15 h 43 min 40 sec | CHABLAIS (ABONDANCE) | 6.5 | 4.60 |

| | | | | |
|---|---|---|---|---|
| 18 June 1968 | 5 h 27 min 36 sec | VAL D'AOSTE (ARNAZ) | 6.5 | 5.10 |
| 18 April 1968 | 19 h 38 min 17 sec | RIVIERA DI PONENTE (DIANO MARINA) | 6 | 4.60 |
| 19 July 1963 | 5 h 46 min 5 sec | MEDITERRANEE (S. IMPERIA) | 7.5 | 6.00 |
| 25 April 1963 | 13 h 36 min 11 sec | VERCORS (MONTEYNARD) | 7 | 4.50 |
| 25 April 1962 | 4 h 44 min 48 sec | VERCORS (CORRENCON-EN-VERCORS) | 7.5 | 5.00 |
| 23 March 1960 | 23 h 8 min 50 sec | VALAIS (BRIG) | 7 | 5.00 |
| 5 April 1959 | 10 h 48 min | UBAYE (ST-PAUL) | 7.5 | 5.30 |
| 15 September 1958 | 16 h 21 min 51 sec | BUGEY (LA BALME-DE-SILLINGY) | 6 | 4.30 |
| 4 May 1958 | 10 h 52 min 45 sec | PIEMONT (VALDIERI) | 6 | 4.70 |
| 30 March 1958 | 16 h 10 min 12 sec | LAC DU BOURGET (CONJUX) | 6.5 | 4.60 |
| 25 March 1957 | 7 h 46 min 10 sec | LIMAGNE (RANDAN) | 6 | 4.30 |
| 20 June 1955 | 4 h 47 min | PIEMONT (PRAZZO) | 7 | 5.20 |
| 12 May 1955 | 14 h 16 min | PIEMONT (STROPPO) | 7 | 4.80 |
| 29 July 1954 | 4 h 42 min 26 sec | VALAIS (MONTANA) | 6.5 | 5.00 |
| 19 May 1954 | 9 h 34 min 55 sec | VALAIS (N-W. SION) | 7 | 5.30 |
| 26 October 1952 | 20 h 30 min | MAURIENNE (ST-ETIENNE-DE-CUINES) | 5 | 4.16 |
| 8 June 1952 | 21 h 26 min 10 sec | BARONNIES (PIERRELONGUE) | 7 | 4.90 |
| 30 November 1951 | 6 h 8 min | HAUT-VERDON (CHASTEUIL) | 7.5 | 5.30 |
| 22 March 1949 | 18 h 45 min | UBAYE (LE LAUZET) | 6 | 4.30 |
| 27 May 1947 | 16 h 57 min | LAC DU BOURGET (JONGIEUX) | 6 | 4.30 |
| 17 February 1947 | 0 h 12 min | PIEMONT (PRAZZO ?) | 7.5 | 5.20 |
| 25 January 1946 | 17 h 32 min 8 sec | VALAIS (CHALAIS) | 7.5 | 5.80 |
| 10 August 1941 | 19 h 20 min | BAS-PLATEAUX DAUPHINOIS (LA COTE-SAINT-ANDRE) | 6 | 4.30 |
| 23 February 1941 | 20 h 18 min | PIEMONT (PRAZZO ?) | 6 | 4.83 |
| 20 March 1939 | 3 h 3 min | PIEMONT (TORRE PELLICE ?) | 5 | 4.30 |
| 8 December 1938 | 7 h 35 min 56 sec | BAS-PLATEAUX DAUPHINOIS (LA SONE) | 6 | 4.30 |
| 18 July 1938 | 0 h 57 min | QUEYRAS (GUILLESTRE) | 6.5 | 4.60 |
| 5 July 1938 | 17 h 30 min | BASSE-DURANCE (MIRABEAU) | 5 | 4.16 |
| 15 February 1938 | 2 h 32 min | EMBRUNAIS (CHATEAUROUX) | 6 | 4.30 |
| 17 December 1937 | 3 h 11 min 20 sec | QUEYRAS (GUILLESTRE) | 6 | 4.30 |
| 30 September 1937 | 12 h | MOYENNE-DURANCE (LURS) | 6 | 4.60 |
| 11 December 1936 | 17 h 25 min 8 sec | PIEMONT (PIGNA) | 6 | 4.60 |
| 17 April 1936 | 3 h 19 min 5 sec | AVANT-PAYS SAVOYARD (FRANGY) | 7 | 4.90 |
| 13 February 1936 | 5 h 14 min | TRICASTIN (LA GARDE-ADHEMAR) | 6 | 4.30 |
| 19 March 1935 | 7 h 27 min 17 sec | EMBRUNAIS (ST-CLEMENT) | 7 | 4.90 |
| 9 December 1934 | 17 h 40 min | TRICASTIN (VALAURIE) | 6 | 4.30 |
| 12 May 1934 | 8 h 21 min 16 sec | TRICASTIN (VALAURIE) | 7 | 4.90 |
| 19 September 1933 | 3 h 46 min | UBAYE (LE LAUZET) | 6.5 | 4.60 |
| 1 May 1932 | 3 h 42 min | MEDITERRANEE (S. MARSEILLE) | 6 | 4.98 |
| 11 December 1927 | 15 h 49 min | PIEMONT (SUSA) | 6 | 5.00 |
| 24 July 1927 | 22 h 15 min | BARONNIES (MALAUCENE) | 7 | 4.90 |
| 21 July 1925 | 12 h 2 min | AVANT-PAYS SAVOYARD (ST-JULIEN-EN-GENEVOIS) | 5 | 4.20 |
| 8 January 1925 | 2 h 44 min 48 sec | JURA SUISSE (ORBE-LIGNEROLLE) | 6.5 | 4.80 |
| 24 September 1924 | 12 h | COMTAT (CADEROUSSE) | 6.5 | 4.60 |
| 26 July 1924 | 6 h 50 min | MONTAGNES DU HAUT-VAR (BEUIL) | 5 | 4.16 |
| 5 April 1922 | 16 h 28 min | BASSE-PROVENCE (CALLIAN) | 5 | 4.34 |
| 28 November 1919 | 21 h 38 min | PIEMONT (LIMONE PIEMONTE) | 5.5 | 4.90 |

| | | | | |
|---|---|---|---|---|
| 22 February 1916 | 9 h 13 min | UBAYE (BARCELONNETTE) | 5 | 4.16 |
| 16 February 1915 | 3 h 15 min | PREALPES DE DIGNE (DIGNE) | 5.5 | 4.38 |
| 26 October 1914 | 3 h 44 min 7 sec | PIEMONT (SACRA DI SAN MICHELE) | 7 | 5.40 |
| 29 July 1913 | 8 h 50 min | MOYENNE-DURANCE (MANOSQUE) | 5.5 | 4.38 |
| 14 May 1913 | 7 h 17 min | MOYENNE-DURANCE (VOLX) | 7.5 | 5.30 |
| 9 February 1912 | 20 h 17 min | EMBRUNAIS (ST-ANDRE) | 6 | 4.30 |
| 27 September 1911 | 14 h 53 min 35 sec | PREALPES DE DIGNE (BARREME) | 5 | 5.03 |
| 31 July 1910 | 20 h 37 min | TREVARESSE (ROGNES) | 5 | 4.16 |
| 19 May 1910 | 18 h 25 min | TREVARESSE (LAMBESC) | 5 | 4.16 |
| 15 May 1910 | 5 h 35 min | TARENTAISE (MOUTIERS) | 5 | 4.16 |
| 11 June 1909 | 21 h 14 min | TREVARESSE (LAMBESC) | 8.5 | 6.00 |
| 17 February 1909 | 16 h 58 min | CHABLAIS (ABONDANCE) | 6 | 4.50 |
| 7 January 1908 | 15 h | TRICASTIN (ROUSSAS) | 5 | 4.16 |
| 13 August 1905 | 10 h 22 min | MASSIF DU MONT-BLANC (CHAMONIX) | 7 | 5.20 |
| 30 May 1905 | 5 h | PIEMONT (FOSSANO) | 6 | 4.80 |
| 29 April 1905 | 1 h 59 min 15 sec | MASSIF DU MONT-BLANC (LAC D'EMOSSON) | 7.5 | 5.10 |
| 10 April 1905 | 10 h | BARONNIES (VAISON-LA-ROMAINE) | 7 | 4.90 |
| 24 January 1905 | 3 h 20 min | FAUCIGNY (BONNEVILLE) | 5 | 4.16 |
| 12 July 1904 | 5 h 31 min | BRIANCONNAIS (BRIANCON) | 7 | 4.90 |
| 3 September 1903 | 8 h 17 min | PIEMONT (BAGNI DI VINADIO) | 5 | 4.99 |
| 4 April 1903 | 2 h | RIVIERA DI PONENTE (ONEGLIA) | 5.5 | 4.60 |
| 13 May 1901 | 8 h 21 min 12 sec | BAS-PLATEAUX DAUPHINOIS (MANAS) | 7 | 4.90 |
| 25 December 1900 | 23 h 15 min | CLUSE DE CHAMBERY (CHAMBERY) | 5.5 | 4.38 |
| 26 December 1899 | 10 h 10 min | PIEMONT (CUNEO) | 5 | 4.37 |
| 29 July 1899 | 0 h 6 min | BASSE-PROVENCE (LES ARCS) | 5 | 4.02 |
| 16 October 1896 | 6 h 30 min | RIVIERA DI PONENTE (ONEGLIA) | 7 | 4.68 |
| 3 February 1893 | | BAS-PLATEAUX DAUPHINOIS (ST-MARCELLIN) | 5 | 4.16 |
| 18 February 1889 | 7 h 30 min | BAS-PLATEAUX DAUPHINOIS (LA TOUR-DU-PIN) | 6.5 | 4.44 |
| 23 February 1887 | 5 h 50 min | RIVIERA DI PONENTE (IMPERIA-BUSSANA) | 9 | 6.62 |
| 4 May 1885 | 7 h 5 min | BASSE-PROVENCE (LES ARCS) | 5 | 4.08 |
| 27 November 1884 | 22 h 57 min | QUEYRAS (GUILLESTRE) | 7 | 5.67 |
| 10 December 1882 | 17 h 40 min | BELLEDONNE-PELVOUX | 5 | 4.49 |
| 25 November 1881 | 18 h 22 min | BAS-VALAIS (AIGLE) | 6 | 4.46 |
| 22 July 1881 | 2 h 45 min | BELLEDONNE-PELVOUX | 7 | 5.72 |
| 30 December 1879 | 12 h 27 min | CHABLAIS (ST-JEAN-D'AULPS) | 7 | 4.97 |
| 9 September 1879 | 7 h 50 min | PLATEAU DE CREMIEU (CREMIEU) | 6 | 5.13 |
| 24 June 1878 | 9 h 18 min | BAS-PLATEAUX DAUPHINOIS (MORAS-EN-VALLOIRE) | 6 | 4.46 |
| 24 June 1878 | 9 h 12 min | BASSE-VALLEE DE LA SAONE (ANSE) | 6 | 4.71 |
| 8 October 1877 | 5 h 12 min | FAUCIGNY (LA ROCHE-SUR-FORON) | 7 | 5.62 |
| 8 August 1873 | 3 h | TRICASTIN (CHATEAUNEUF-DU-RHONE) | 7 | 4.66 |
| 2 December 1872 | | PREALPES DE DIGNE (DIGNE) | 5 | 4.16 |
| 20 June 1872 | | TRICASTIN (LA GARDE-ADHEMAR) | 6.5 | 4.45 |
| 23 March 1868 | 20 h 30 min | CAMARGUE (ARLES) | 5 | 4.52 |
| 22 September 1866 | 15 h | PIEMONT (PINEROLO) | 5.5 | 4.48 |
| 19 May 1866 | 9 h 12 min | LARAGNE (LA MOTTE-DU-CAIRE) | 7.5 | 5.59 |
| 25 December 1865 | 22 h | CHABLAIS (LE BIOT) | 5 | 4.16 |
| 4 January 1865 | | PLAINE DE VALENCE (GRANE) | 5 | 4.16 |

| | | | | |
|---|---|---|---|---|
| 8 December 1863 | 3 h 50 min | COMTAT (L'ISLE-SUR-LA-SORGUE) | 6 | 4.13 |
| 18 November 1862 | 7 h | PLATEAU DE VALENSOLE (GREOUX-LES-BAINS) | 5 | 4.16 |
| 20 December 1861 | 8 h 30 min | PIEMONT ? | 6 | 4.52 |
| 17 December 1858 | 8 h 30 min | BASSE-DURANCE (MIRABEAU) | 6 | 4.20 |
| 6 August 1858 | 2 h 30 min | RIVIERA DI PONENTE (ONEGLIA) | 5 | 5.10 |
| 27 December 1856 | 1 h 30 min | VERCORS (CHATEAUDOUBLE) | 6 | 4.33 |
| 12 December 1855 | 20 h 40 min | HAUT-VERDON (CHASTEUIL) | 8 | 5.21 |
| 25 July 1855 | 12 h 50 min | VALAIS (VISP) | 9 | 6.06 |
| 12 May 1855 | 22 h 20 min | COSTIERE (ST-GENIES-DE-COMOLAS) | 5 | 4.21 |
| 29 December 1854 | 3 h 10 min | RIVIERA DI PONENTE (SAN REMO) | 7.5 | 6.32 |
| 22 November 1852 | 13 h | TRICASTIN (DIEULEFIT) | 6.5 | 4.45 |
| 24 August 1851 | 2 h | OBERLAND (S-W. THUN ?) | 7 | 4.82 |
| 1 October 1849 | 0 h 30 min | MAURIENNE (BONVILLARD) | 6 | 4.17 |
| 30 November 1847 | 6 h 30 min | PLAINE DE VALENCE (ROMANS-SUR-ISERE) | 5.5 | 4.32 |
| 12 December 1846 | 10 h 15 min | BASSE-PROVENCE (GEMENOS) | 6 | 4.44 |
| 10 December 1844 | 1 h | CHAUTAGNE ? | 5 | 4.08 |
| 2 December 1841 | 19 h 53 min | ALBANAIS (RUMILLY) | 6.5 | 5.14 |
| 11 August 1839 | 20 h | AVANT-PAYS SAVOYARD (ANNECY) | 7 | 4.32 |
| 3 April 1839 | 18 h 30 min | GRESIVAUDAN (DOMENE) | 6 | 4.30 |
| 22 May 1838 | 7 h | VERCORS (MEAUDRE) | 6.5 | 4.45 |
| 7 March 1835 | 6 h | BASSE-DURANCE (BEAUMONT-DE-PERTUIS) | 6 | 4.44 |
| 9 October 1828 | 3 h 15 min | APENNINS LIGURES (VOGHERA) | 8 | 5.71 |
| 23 May 1824 | 13 h | HAUT-VERDON (CASTELLANE) | 5 | 4.16 |
| 13 December 1823 | 3 h | BUGEY (BELLEY) | 5.5 | 4.30 |
| 19 February 1822 | 8 h 45 min | BUGEY (BELLEY) | 7.5 | 5.52 |
| 23 February 1818 | 19 h | RIVIERA DI PONENTE (ONEGLIA) | 7 | 5.48 |
| 11 March 1817 | 21 h 25 min | MASSIF DU MONT-BLANC (CHAMONIX) | 7 | 5.59 |
| 20 March 1812 | 0 h 1 min | BASSE-DURANCE (BEAUMONT-DE-PERTUIS) | 7.5 | 4.86 |
| 13 March 1809 | | VERCORS (BOUVANTE) | 6 | 4.20 |
| 2 April 1808 | 17 h 45 min | PIEMONT (TORRE PELLICE) | 8 | 5.44 |
| 5 September 1807 | 1 h 30 min | RIVIERA DI PONENTE (SAN-REMO) | 5.5 | 4.84 |
| 20 June 1806 | 23 h 15 min | COTE D'AZUR (NICE) | 6 | 4.20 |
| 20 January 1806 | 0 h 15 min | ALPILLES (ORGON) | 5 | 4.16 |
| 5 March 1799 | 4 h | COTE D'AZUR (NICE) | 5 | 4.16 |
| 12 September 1785 | 0 h 15 min | PIEMONT (VAL DE SUSA. OULX) | 7 | 4.44 |
| 29 April 1785 | 10 h 45 min | QUEYRAS (MONT-DAUPHIN) | 6 | 4.17 |
| 15 October 1784 | 12 h 3 min | LAC DU BOURGET (AIX-LES-BAINS) | 6.5 | 5.16 |
| 6 July 1783 | 9 h 56 min | VALLEE DE L'OUCHE (BLIGNY) | 6 | 5.14 |
| 25 March 1783 | 3 h | BASSE-DURANCE (MALLEMORT) | 5 | 4.44 |
| 15 August 1782 | 16 h | BELLEDONNE (URIAGE) | 6 | 4.12 |
| 31 December 1773 | 1 h 15 min | QUEYRAS (GUILLESTRE) | 6 | 4.44 |
| 7 February 1773 | 1 h 45 min | TRICASTIN (CLANSAYES) | 6 | 4.58 |
| 11 June 1772 | 5 h | TRICASTIN (CLANSAYES) | 5.5 | 4.20 |
| 21 December 1769 | 14 h 30 min | COMTAT (BEDARRIDES) | 7 | 4.18 |
| 18 November 1769 | 4 h | COMTAT (BEDARRIDES) | 7 | 4.40 |
| 8 July 1766 | 15 h | BRIANCONNAIS (BRIANCON) | 5 | 4.16 |
| 12 July 1763 | 7 h | LUBERON OCCIDENTAL (MENERBES) | 6.5 | 4.88 |

| | | | | |
|---|---|---|---|---|
| 5 May 1762 | 21 h 28 min | BAS-PLATEAUX DAUPHINOIS (LA VERPILLIERE) | 6 | 4.46 |
| 28 August 1756 | 5 h 30 min | COMTAT (CARPENTRAS) | 5 | 4.16 |
| 3 July 1756 | 2 h 20 min | BASSIN D'AIX-EN-PROVENCE (AIX-EN-PROVENCE) | 6 | 4.20 |
| 9 December 1755 | 14 h 45 min | VALAIS (BRIG) | 8.5 | 5.74 |
| 12 January 1754 | 22 h | CHARTREUSE (VOREPPE) | 6.5 | 4.71 |
| 29 August 1740 | 0 h 30 min | COTE D'AZUR (ANTIBES) | 5 | 4.16 |
| 18 October 1738 | 16 h 15 min | COMTAT (CARPENTRAS) | 6 | 4.44 |
| 28 October 1730 | 7 h 45 min | CAMARGUE (ARLES) | 6.5 | 4.45 |
| 27 May 1727 | 1 h 45 min | CAMARGUE (ARLES) | 6.5 | 4.17 |
| 11 June 1719 | 2 h | BARONNIES (MOYDANS) | 5.5 | 4.17 |
| 14 August 1708 | 6 h 15 min | MOYENNE-DURANCE (MANOSQUE) | 8 | 5.03 |
| 21 March 1708 | 23 h | MOYENNE-DURANCE (MANOSQUE) | 5.5 | 4.17 |
| 12 December 1693 | 20 h | COMTAT (TARASCON-SUR-RHONE) | 5 | 4.16 |
| 31 August 1684 | 23 h 55 min | PREALPES DE DIGNE (DIGNE) | 5.5 | 4.38 |
| 2 September 1678 | 3 h | MOYENNE-DURANCE (MANOSQUE ?) | 7 | 4.55 |
| 20 March 1649 | | BAS-PLATEAUX DAUPHINOIS (BEAUREPAIRE) | 5.5 | 4.13 |
| 15 February 1644 | 4 h 30 min | ALPES NICOISES (ROQUEBILLIERE) | 8 | 5.76 |
| 26 December 1624 | 23 h | BRIANCONNAIS (BRIANCON) | 5 | 4.16 |
| 1 February 1622 | | CRAU (SALON-DE-PROVENCE) | 6 | 4.20 |
| 18 January 1618 | 5 h | ALPES NICOISES (COARAZE) | 8 | 5.32 |
| 31 January 1612 | 15 h | RIVIERA DI PONENTE (LOANO) | 7.5 | 4.77 |
| 3 January 1610 | 18 h | BASSIN DE MONTELIMAR (MONTELIMAR) | 5 | 4.16 |
| 28 December 1590 | 22 h | QUEYRAS (CHATEAU-VILLE-VIEILLE) | 5 | 4.16 |
| 11 March 1584 | 11 h 30 min | LAC LEMAN (MONTREUX) | 7 | 5.80 |
| 20 May 1578 | 16 h | BAS-PLATEAUX DAUPHINOIS (LA TOUR-DU-PIN ?) | 6.5 | 4.68 |
| 20 July 1564 | 20 h | ALPES NICOISES (LA BOLLENE-VESUBIE) | 8 | 5.50 |
| 4 May 1549 | 22 h | BASSIN DE MONTELIMAR (MONTELIMAR) | 6 | 4.20 |
| 13 December 1509 | 11 h | MOYENNE-DURANCE (MANOSQUE) | 8 | 5.54 |
| 23 June 1494 | | ALPES NICOISES (ROQUEBILLIERE) | 8 | 4.72 |
| 26 May 1397 | 23 h 55 min | CAMARGUE (ARLES) | 5.5 | 4.17 |